The role of inorganic nutrients and dissolved organic phosphorus in the phytoplankton dynamics of a Mediterranean Bay. A modeling study.

Clara Llebot*[,a], Yvette H. Spitz[b], Jordi Solé[a], Marta Estrada[a]

[a] *Institut de Ciències del Mar, CSIC. Passeig Marítim de la Barceloneta 37–49 08003 Barcelona, Spain*

[b] *College of Oceanic and Atmospheric Sciences, Oregon State University. 104 COAS Administration Building, Corvallis, OR, USA*

Abstract

The effect of Dissolved Organic Phosphorus (DOP) availability and nutrient-limitation of phytoplankton growth in an estuarine Mediterranean bay (Alfacs Bay, NW Mediterranean) have been studied by means of a zero-dimensional ecological model including nitrogen, phosphorus, two groups of phytoplankton (diatoms and flagellates), one group of zooplankton, and detritus. Simulations with and without DOP as an extra source of phosphorus for phytoplankton growth suggest that DOP plays an important role in the dynamics of the Alfacs Bay ecosystem. DOP uptake by phytoplankton is indeed necessary to simulate the observed draw-down of nitrate and build-up of phytoplankton biomass. It also leads to phosphorus limitation of phytoplankton growth in the winter and nitrogen limitation in spring and summer, which is in agreement with observations. Simulations with and without sediment resuspension suggest that sediment resuspension does not significantly affect the nitrogen budget in the bay.

Key words: Spain, Catalunya, Alfacs Bay; Mediterranean Sea; Dissolved Organic Phosphorus; Resuspended Sediments; Ecological Modelling; Marine Ecology; Limiting factors;

*Corresponding author

Email addresses: llebot@icm.cat (Clara Llebot), yvette@coas.oregonstate.edu (Yvette H. Spitz), jsole@icm.cat (Jordi Solé), marta@icm.cat (Marta Estrada)

1. Introduction

Coastal regions are highly dynamic and productive areas that have historically attracted human populations. In the confluence between a river mouth and the sea, estuaries are composed of a variety of habitats and have both a high ecological and economical value. Such areas sustain nutrient cycling, provide shelter and nursery grounds for many aquatic species, and support successful fisheries and aquaculture activities.

A major challenge in the study of marine coastal areas is understanding the interactions among physico-chemical variables and the ecosystem behavior. Physical forcing, such as freshwater discharge, tidal currents, or mixing due to barotropic or baroclinic processes can play a key role in the evolution of the ecological dynamics of the communities of a coastal area. In the Mediterranean, coastal systems are characterized by the absence of a strong tidal signal. We chose Alfacs Bay, in the Ebre Delta (NW Mediterranean) to address question of nutrient cycle and plankton growth. This bay, which is characterized by no tidal forcing and by human controlled freshwater discharge, presents a complex interplay among physical, chemical and biological variables

The mouth of the Ebre river, one of the largest rivers discharging into the NW Mediterranean, forms a flat arrow-shaped delta that encloses two shallow bays: Fangar to the north, and Alfacs, the largest one, to the south (Fig. 1). The bays are 4 and 6 m deep and are subject to the typically small tides of the Mediterranean (not greater than 0.2 m). They are highly productive, and host successful aquaculture businesses (Camp and Delgado, 1987; DAAAR, 2008). However, algal blooms - some of them harmful - have been recurrent in Fangar and Alfacs since 1989 (Delgado et al., 1990). Their frequency has increased over the years, just as it has increased in other harbors of the neighboring Catalan coast (Vila et al., 2001).

Harmful algal blooms (HAB) consist of different species, such as the dinoflagellates *Alexandrium minutum* (Delgado et al., 1990), *Dinophysis sacculus* (Garcés et al., 1997) and *Karlodinium spp* (formerly identified as *Gyrodinium corsicum*) (Fernández-Tejedor et al., 2004; Garcés et al., 1999), or diatoms of the genus *Pseudonitzschia* (Quijano-Sheggia et al., 2008). Some of these proliferations are associated with massive mortalities of cultured fish, mussels (*Mytillus galloprovincialis*) and natural fauna in the bay. Because these blooms consist primarily of flagellates or diatoms, the dynamics of the populations of these groups will be one of the foci of this study.

In recent years, few field and modelling studies have addressed the linkage between the phytoplanktonic community and the physics of Alfacs Bay, from both a mesoscale (Llebot et al., 2008) and microscale (Artigas, 2008) point of view, some of them focusing specially on HABs (Artigas, 2008). In spite of this work, a good understanding of the main physico-chemical factors controlling the phytoplankton communities in the bay is still lacking. Phytoplankton growth is affected by a large number of variables, such as nutrients, light, temperature, grazing and advection. Several studies have documented the variability of temperature, water

transport and other physical properties in Alfacs Bay (Camp, 1994; Llebot, 2007; Solé et al., 2009). Because of its shallowness, primary production in Alfacs is not likely to be heavily light-limited. In this context, one of the most challenging questions concerning the ecology of Alfacs Bay is the role of nutrient fluxes on phytoplankton community succession, and bloom development.

The main sources of dissolved inorganic nutrients in Alfacs Bay are freshwater discharges from irrigation channels and treatment plants, ground water inputs, exchanges with the open ocean through the mouth of the bay, fluxes from sediments, and recycling and remineralisation from biological processes. Agricultural practice in the Ebre Delta, which is dominated by rice farming, delivers high-nitrogen nutrient loads to the bay through freshwater channels. In general June and October are the months with higher nutrient concentration in the channels, because the fields are fertilized in June and emptied in October after the crop (Muñoz, 1998). In addition to drainage channels, ground water seepage appears to be also an important source of nutrients, given the high nitrate concentrations in the Ebre Delta aquifers (Ministerio de Obras Públicas, Transportes y Medio Ambiente; Ministerio de Industria y Energía, 1995; Torrecilla et al., 2005). The sinks of nutrients occur mainly via advection and consumption by phytoplankton and other organisms, which can produce detrital matter sinking to the sediment.

Although some decades ago phosphorus was considered to be a major eutrophication agent, it is now being recognized that nitrogen, which is widely used as a fertilizer, is the main pollutant affecting coastal waters worldwide (Howarth and Marino, 2006). This observation would suggest a limiting role for phosphorus. However, spatial and seasonal heterogeneity in nutrient loadings have led to complex variability among the limiting nutrients in many estuaries around the world (D'Elia et al., 1986; Fisher et al., 1992; Malone et al., 1996).

The question of the nutrient control of phytoplankton growth in Alfacs Bay has been addressed by several studies. Delgado and Camp (1987) reported a N:P ratio between 0.1 and 4.5 and concluded that nitrogen was the limiting nutrient of the system, as for many coastal areas. They suggested that the transport of nitrogen and phosphorus from the bottom was an essential process in the high productivity of Alfacs Bay. Forès (1989) observed high retention of both nitrogen (26 - 87 %) and phosphorus (13 - 82 %) by the rice fields, and stated that the bays received phosphorus-depleted water, since P was the element most readily assimilated by the rice fields. Assuming nitrogen limitation, Forès (1989) claimed that phosphorus retention would be unlikely to have a negative effect on the productivity of the bays. However, later works pointed to a more complicated hybrid situation in which phosphorus and nitrogen alternate their limiting status depending on the season and on the specific physical conditions of the water column (e.g. sediment resuspension). Vidal (1994) found that inorganic phosphorus in the bay remained considerably stable throughout the year, due to a buffer mechanism activated by sediments resuspension. They considered phosphorus as the main limiting nutrient,

but the type of limitation was a changing feature of the system, in which atmospheric and hydrodynamic forces could play a key role. Cruzado et al. (2002) also concluded that phosphorus was the limiting nutrient in the Ebre Delta system, arguing that the largest nutrient load to the coastal environment corresponded to nitrogen. However, Quijano-Sheggia et al. (2008) indicated that NO_3^- and NH_4^+ were the principal variables affecting the composition of the phytoplankton community in Alfacs Bay. This suggests, therefore, that there would be nitrogen limitation.

Our hypothesis is that nutrient limitation of phytoplankton production in Alfacs changes over the year, with phosphorus or nitrogen limiting during different periods, depending on the variability of the sources and sinks of both nutrients. In particular, we will focus on two processes affecting phosphorus limitation: 1) phosphorus release from the sediment after a resuspension event due to wind stirring (Vidal (1994)); 2) the ability of flagellates and other phytoplankton to use DOP as a source of P. Although this second possibility has been shown by several experimental studies (Bentzen et al., 1992; Currie and Kalff, 1984; Huang and Hong, 1999; Johannes, 1964; Oh et al., 2002; Yamamoto et al., 2004) it is only rarely taken into account by ecological models. Recent studies of Alfacs Bay have associated DOP inputs with freshwater discharges and have shown that it can reach higher concentrations than inorganic phosphorus during a large part of the year (Loureiro et al., 2009).

The general aim of this work is to ascertain, by means of an ecosystem model, which nutrient or nutrients potentially limit phytoplankton production in Alfacs and to describe the main sources and sinks of these nutrients and how they affect the phytoplankton community composition. We will test two main hypotheses: 1) nitrogen and phosphorus limit phytoplankton growth and affect its composition during different seasons and 2) this alternation can be explained by two processes that affect phosphorus availability, in addition to freshwater inputs: the release of phosphorus by sediment resuspension, and the capacity of phytoplankton to use dissolved organic phosphorus as a source of phosphorus.

In order to approximate the budgets and fluxes of nitrogen and phosphorus and to answer the above questions, we built a 0-dimensional ecological model of the estuarine mixed layer. The model includes seven state variables: zooplankton, flagellates, diatoms, dissolved inorganic nitrogen, dissolved inorganic phosphorus, detrital phosphorus, and detrital nitrogen. The forcing variables are water density, wind intensity and freshwater inputs, in addition to DOP and Si that will be introduced into the model based on a time series of measured concentrations.

In section 2, Materials and Methods, we present the model equations and parameter values, and the choice of initial conditions and forcing used in the simulations. We also describe field data. The results section (section 3) contains the results of the various simulations using different sets of assumptions about the occurrence of sediment resuspension and the possibility of DOP utilization by phytoplankton, and presents

the comparisons of these results with measured data. These results are discussed in section 4. Finally, we summarize and conclude our study in section 5.

2. Materials and Methods

2.1. Study site

Alfacs Bay (Fig. 1) is the most southern bay of the Ebre River deltaic complex (40°33'–40°38'N, 0°33–0°44'E), and also the largest. It is roughly 11 km long and 4 km wide; its average depth is 3.13 m and the maximum depth is 6.5 m; its volume is approximately 153×10^6 m^3 of water. A sand barrier separates the basin from the sea. The mouth of the bay is about 2.5 km wide allowing water to be exchanged with the open sea (Camp, 1994).

2.2. The model

The model used in this study is a zero dimensional mixed layer model that describes the nitrogen and phosphorus fluxes of a shallow non-tidal estuarine bay. The temporal rate of change of any variable of the model follows the equation:

$$\frac{\partial C}{\partial t} = Q_{(C)}, \tag{1}$$

where C is any variable in the model, and $Q_{(C)}$ represents the sources minus sinks of the model variable.

The mixed layer deepening and shallowing are calculated using buoyancy and wind stress. The model considers horizontal advection due to exchanges with the open sea across the mouth of the bay, and to freshwater inputs from channels and underground seepage. Advection is included in the $Q_{(C)}$ term. Diffusion is not taken into account in this simple model.

The dynamics of the state variables, Zooplankton (ZOO), Diatoms (PH1), Flagellates (PH2), Dissolved Inorganic Nitrogen (DIN), Dissolved Inorganic Phosphorus (DIP), Detrital phosphorus (DTP) and Detrital nitrogen (DTN) are described by equations 4 to 8 in Table 1. Both groups of phytoplankton are grazed by one generic group of zooplankton. The growth of flagellates and diatoms is limited by nutrients and light. In addition to DIN and DIP, nutrients include silicon (Si) (for diatom growth) and Dissolved Organic Phosphorus (DOP), that are imposed in the model based on monthly averages of observations carried out between April 2007 and March 2008 (Loureiro et al., 2009). Dead phytoplankton cells go to the detritus pool, as do dead zooplankton and the fraction of grazed phytoplankton that is not assimilated. Detritus pools have a loss by sedimentation and are remineralized to inorganic nitrogen and phosphorus, that also receive

inputs from zooplankton excretion. Inorganic nutrients are available for phytoplankton uptake. See Fig. 2 for a general view of the model and Table 2 for a description of the model parameters. The model is forced by six variables: water density, DOP, silicon, wind, rainfall, and freshwater inputs, which include discharge from channels and underground waters (Fig. 3, Table 3).

2.2.1. Physical processes

2.2.1.1. Mixed Layer Depth.

The mixed layer depth represents the depth range through which surface fluxes have been mixed in the recent past. It can be defined by a difference in temperature or density from the surface, or by a gradient in temperature or density (Brainerd and Cregg, 1995). Because of the lack of continuous profiles of density or temperature, we estimated the mixed layer depth using the Richardson Number. The Richardson Number indicates the potential mixing of an estuary and can be calculated as the ratio between buoyancy due to differences of density and the kinetic energy due to the wind. Fisher et al. (1979) define four regimes (A, B, C and D) that range from weak wind forcing and strong stratification (regime A) to strong wind forcing, causing a well mixed column (regime D). The range of winds and water densities in Alfacs suggests a transition between regime B and C when the wind is stronger than 5 m/s (Llebot, 2007). Regime B is characterized by internal waves and a sharp thermocline, while regime C has a mixed column, and a longitudinal temperature gradient. The transition between regime B and C is defined by Fisher et al. (1979) to be at $Ri = (L/2h)^2$ By substituting this value into the Richardson Number expression, we obtained equation 26 (Table 4), with which we calculated an approximation of the mixed layer depth for the model runs. Results were filtered with a 48h filter (Fig. 3).

2.2.1.2. Advection terms.

These include the water fluxes across the mouth of the bay and the freshwater inputs.

Fluxes across the mouth of the bay: This component, called $\mathrm{Advection}$ in the equations of Table 1, represents the flux of mixed layer water in and out of the bay and is assumed to depend only on the wind speed. Although these advection exchanges could be affected by other factors, such as patterns of circulation or density differences between the surface and bottom layer, the lack of data led us to use this formulation as a first approximation. The fact that the model is simulating only the behavior of the mixed layer makes this assumption more realistic, although we are aware of its limitations. At present, there are current-meters in the bay that will alleviate this uncertainty in the near future.

It is reasonable to assume that the Ekman surface velocity (equation 23, Table 4) applies to the whole mixed layer in Alfacs Bay because of the shallowness of the bay. The velocity at a depth of 3 m would

be $v_3 = 0.9996\ v_0$. We then calculate the speed and direction of the currents using equation 23 (Table 4), taking into account that the direction of the surface flow is at a 45 degree angle to the right of the wind direction. In order to calculate the advection, we are only interested in the currents that move the water in and out of the bay, that is, the direction parallel to the coast. By using a principal component analysis of currents at the center of the bay (Artigas, 2008) showed that the dominant current directions are parallel to the coast (East direction -15 degrees) and perpendicular to the coast (North direction -15 degrees). The calculation of $\mathrm{Advection}$ with equations 21 and 22 (Table 4) is performed using the component of the current velocity that corresponds to the East direction (- 15 degrees). The results are shown in Fig. 3.

For the advection calculations, it is assumed that oceanic concentrations of organisms and detritus are zero, and the concentration of DIP and DIN are approximated using data from the FAN cruises (Salat et al., 2002). Low DIP and DIN concentrations are used for the spring, summer and fall months, while the winter concentrations are three times the other month concentrations (Table 2).

Freshwater inputs: Freshwater inputs ($\mathrm{FWInput}$) enter the bay by two different means: discharge channels from rice fields and underground water seepage. We consider that the only non negligible scalars carried by freshwater are nitrogen and phosphorus. Freshwater sources from water treatment plants have not been included, because they only represent roughly 0.01% of the land inputs (Camp, 1994). See section 2.3 for information about the fluxes and equation 24 (Table 4) for details about the calculation.

2.2.2. Biogeochemical processes

2.2.2.1. Growth.

Phytoplankton growth in this model is controlled by light and nutrients (equations 9 and 10, Table 4). There is no temperature limitation.

Light limitation: Many mathematical expressions have been proposed to relate the primary productivity to irradiance (I). Most of them (Jassby and Platt, 1976; Platt et al., 1980) use two common parameters: the slope of the light-saturation curve at low light levels (α), and the maximum specific photosynthetic rate (P_m^B). As the curves obtained are very similar, we chose one of the simplest equations (Table 4, equation 12), from Smith (1936).

The variable I in equation 12 (Table 4) is the irradiance received by the cell and is calculated from equation 13 (Table 4), which uses the incoming solar radiation I_0, the percentage of Photosinthetically Active Radiation (PAR), albedo (θ), and day length (Matlab program from Fennel and Neumann (2004)). As our model is zero-dimensional, depth dependence was not taken in account. The photosynthetic parameters (Table 2) of equation 13 (Table 4) are taken from Fennel et al. (2002).

Nutrient uptake: Nutrient uptake is parameterized using a colimitation equation (Lancelot et al., 2005; O'Neill et al., 1989). Total phosphorus (P) is the sum of DIP and DOP (Table 4, equation 14). Diatoms are limited by nitrogen, phosphorus and silicon (Table 4, equation 15), while flagellates are only limited by nitrogen and phosphorus (Table 4, equation 16).

The maximum growth rate and mortality of phytoplankton and zooplankton are initialized following Lacroix and Nival (1998), and then calibrated by means of recursive simulations, keeping the values within the usual ranges for ecological models (Chapelle et al., 2000; Giraud, 2006; Kishi et al., 2007; le Quéré et al., 2005; Lima et al., 2002; Merico et al., 2004; van den Berg et al., 1995). The maximum growth rate for diatoms is higher than the maximum growth rate for flagellates, as in Kishi et al. (2007), Lacroix and Nival (1998) or Merico et al. (2004). The half saturation constants for DIN uptake are taken from Fennel et al. (2002). The half saturation constant for flagellates is set lower, meaning that this group has a higher affinity for the substrate, as in Lacroix and Nival (1998); Merico et al. (2004) or Crispi et al. (2002). The half saturation constants for DIP uptake are taken from Tyrrell (1999), and modified according to the range measured by Taft et al. (1975). The half saturation constant for silicon uptake is taken from Kishi et al. (2007) and slightly modified in order to agree better with observations. The half saturation constant for DOP is within the ranges measured in Bentzen et al. (1992) for bacteria and is similar to the values used in other models including DOP (Chen et al., 2002).

2.2.2.2. Nutrient sources.

Dissolved Organic Phosphorus: The DOP has been added as a source of phosphorus in the model. The origin of DOP can be excretion from living bacteria, plants and animals, or decomposition from dead organisms. A large proportion of the DOP is formed by high molecular weight or colloidal material that is not readily available for uptake. Phytoplankton and bacteria can use some organic P substrates by the action of phosphomonoesterase enzymes. The most widely recognized of these enzymes in aquatic systems is the nonspecific alkaline phosphatase (Bentzen et al., 1992). It has been seen that, particularly in situations of phosphorus stress, phytoplankton have a notable capacity for phosphorus uptake from organic sources (Currie and Kalff, 1984).

DOP is imposed in the model using the observations from Loureiro et al. (2009), since we consider that a large portion of the DOP comes from freshwater inputs and rice fields. Because the entire pool is not available for phytoplanktonic use, only a fraction of this pool is considered (see Table 2). In the colimitation equation used for the calculation of the nutrient uptake (Table 4, equation 14) the phosphorus is entered as the sum of DIP and DOP (Table 4, equations 15 and 16), and a common half saturation constant for phosphorus is used (Table 2). In order to calculate the proportion of phosphorus used from the DIP pool

(named $\mathrm{Growth\_eq}_{(\mathrm{PHX})}$ in Table 1) and from the DOP pool, we use equation 11 (Table 1), following Spitz et al. (2001).

Sediment resuspension: Theoretically, the adsorption/desorption reactions that take place in the sediment can have an important influence on the total concentration of dissolved inorganic phosphorus in the water column (Froelich, 1988; Lebo, 1991). Vidal (1994) studied the phosphate dynamics tied to sediment disturbances in Alfacs. She found a buffering effect that leads to a final concentration of about 0.2 to 0.3 mmol P m^{-3} of soluble reactive phosphorus (SRP) when the sediments are resuspended. However, if the sediments were not resuspended but just gently stirred, the SRP concentration was undetectable. In the model, we assumed that sediment resuspension occurs when the mixed layer depth reaches the bottom. In this case, there is a flow of phosphorus (DIP) from the sediment to the water column during the first 30 minutes. After this 30 minute period, an equilibrium concentration is reached due to the buffering system described in Vidal (1994). The amount of phosphorus released during resuspension and the equilibrium concentration were fixed using the data in Vidal (1994) (see Table 2).

2.2.2.3. Zooplankton grazing.

As Franks (2002) states in his review of NPZ models, representation of zooplankton grazing has always presented a complex problem. The formulation can include a saturating response to increasing food, grazing thresholds, varying degrees of nonlinearity and acclimation of the grazing rate to changing food conditions. We used a saturating formulation with preferences of grazing as in Fasham et al. (1990) (see equation 19 and 20, Table 4).

About 90 rafts devoted to mussel cultivation are located in Alfacs Bay. However, filtering by mussels was not included explicitly in the model, because the global impact on chlorophyll concentration in the bay was estimated to be less than 1% per day.

2.2.2.4. Other formulations.

Mortality of both zooplankton and phytoplankton is expressed by a mortality rate m (Table 4 equation 32). However, as seen in equations 2, 3 and 4 (Table 1), death terms are linear for phytoplankton but quadratic for zooplankton (see an example in Kishi et al. (2007)). *Excretion* is parameterized linearly with an excretion rate E (Table 4, equation 33). *Remineralisation* is controlled by a remineralisation rate (Table 4, equation 34). *Sedimentation* is expressed with a sinking velocity using equation 28 (Table 4).

2.3. Forcing variables

See Table 3 for a summary of the forcing variables, and Fig. 3 for graphs of the data. *Density* is taken from a climatology calculated with 14 years of field data (Solé et al., 2009). *Dissolved organic phosphorus* and *Silicon* are obtained from Loureiro et al. (2009). They calculated monthly averages based on weekly samples taken between April 2007 and March 2008, from surface water (0.5 m depth) at a station located in the center of Alfacs Bay (40° 36' 0"N, 0° 39' 0" E). An annual composition of these data is shown in Fig. 3. *Wind speed and direction* are obtained from an automatic weather station (named Els Alfacs) managed by the Meteorological Service of Catalonia (SMC) located on the north shelf of the bay (UTM X 302380, UTM Y 4500160; see Fig. 1). Monthly accumulated *rainfall* climatology is calculated using daily data from the National Institute of Meteorology. The station, Roquetes (Tortosa) is located 10 km north from the bay, next to the Ebro River, and the data set includes data from 1990 to 2004. A cubic spline interpolation was performed to fit the data set to the time step used in the model.

Forcing by freshwater inflow includes *discharge channel flux* and the *underground water inputs*. Freshwater enters Alfacs Bay from a network of controlled drainage channels coming from the rice fields. Rice is cultivated on 57% of the surface of the Ebre Delta (about 7880 Ha), in lands flooded to a depth of 15-20 cm (Farnós et al., 2007). The growing season lasts approximately 190 days, from the beginning of April to the end of September. Rice is planted as a seed a week after flooding, which is followed by a vegetative period (95 days), a reproductive period (20 days) and a ripening period (40 days) (Forès and Comín, 1992). During these periods the freshwater flux to the bays is maximum (1.84 dm^3 s^{-1} Ha^{-1}). Since 2001, a lower flux from the channels (1 dm^3 s^{-1} Ha^{-1}) is maintained after the crop for agroenvironmental reasons. This situation lasts about 120 days, from October to mid January. Finally, from mid January to the end of March, the channels are closed, and the discharge channel flux is 0. When the water starts flowing again, all the fields are flooded with 15 cm of water in 10 days. The distribution of the channel freshwater discharge during the year is shown in Fig. 3.

Nutrient concentration in the waters entering the bay is one of the most important values that needs to be specified. It was approximated as follows. The nitrate concentration measured in the channels ranges from 20 to 80 mmol N m^{-3} in Muñoz (1998) and from 15 to 45 mmol N m^{-3} in Camp and Delgado (1987). de Pedro (2007) reported that the average nitrate concentration changed from 29.8$\pm$7 mmol N m^{-3} in 1986-1987 to 85.3$\pm$16 mmol N m^{-3} in 1996-1997. Nitrite values vary from 2 to 14 mmol N m^{-3} (Muñoz, 1998) and from 1.6 to 2.8 mmol N m^{-3} (Camp and Delgado, 1987), and changed from 3.34$\pm$1 mmol N m^{-3} in 1986-1987 to 6.35$\pm$2 mmol N m^{-3} in 1996-1997 (de Pedro, 2007). Values for ammonium are 10 - 100 mmol N m^{-3} (Muñoz, 1998), and 19.3$\pm$5 and 76.1$\pm$29 in 1986-1987 and 1996-1997, respectively. Given the high variability of the nitrogen concentration in the channels and the lack of data to assess its potential

temporal dependence, a constant value of 70 mmol N m^{-3} is adopted. The case for phosphorus is similar, but even less data are available. Phosphate measurements range from 0.8 to 1.5 mmol P m^{-3} (Camp and Delgado, 1987), and the averages reported by de Pedro (2007) decreased from 1.03±0 mmol P m^{-3} for the period 1986–1987 to 0.603±0 mmol P m^{-3} for 1996–1997. A constant value of 0.5 mmol P m^{-3} is chosen as the DIP concentration in the freshwater input.

The *underground inputs of freshwater* were suggested to be 0.7 m^3 s^{-1} by Camp (1994). However, recent modelling studies have shown that this value is probably underestimated (Llebot, 2007). Because of the lack of data we approximate the underground input of freshwater as follows. The minimum flow is fixed to 1.4, doubling the potentially underestimated measure of Camp (1994). As the underground flow may vary depending on the rainfall (Boyle, 1994; Smith et al., 2008), it is assumed that the flow in the wet season doubles the flow in the dry season (as, for example, in Stalker et al. (2009)), following a linear trend.

There are very few observations of the concentration of nutrients in the underground water emptying into Alfacs Bay. Public records of underground water nitrate concentration at various locations in the area of the Ebre Delta (Agència Catalana de l'Aigua, available online), range from 20 mmol m^3 to 3000 mmol m^3. We chose a reasonable value of 500 mmol m^3. As we do not know the phosphate concentration in these waters, we assume that it is the same as in the freshwater channels. Phosphate concentrations found by Torrecilla et al. (2005) in underground waters in other regions of the Ebre river are of the same magnitude.

The initial conditions for the model variables are taken from the January observations for dissolved inorganic nitrogen, dissolved inorganic phosphorus, and diatoms. A first aproximation is used for flagellates, detritus and zooplankton. See Table 5 for the adopted values.

2.4. Sensitivity analysis

A sensitivity analysis was performed in order to evaluate the response of the model parameters that are poorly constrained, i.e. the freshwater fluxes (underground and discharge channels) and their DIP and DIN concentrations. A "one-at-a-time" methodology, which consists of varying one variable while holding the others fixed (Fasham, 1995; Hamby, 1994) is used. The analysis was performed for freshwater fluxes (discharge channels and underground waters) and their DIP and DIN concentrations.

A set of three runs of a simulation that includes the use of DOP by phytoplankton and the resuspension of sediments (*Standard Simulation*) is carried out for each parameter tested (see section 3). Each set of three runs included a simulation with the basic parameter values (as explained in the methods section) (results shown in Figs. 4, 5 and 6, named as *Standard Simulation*) and simulations with an increase and a decrease of 10% of the original value. The standard deviation of these three simulations over one year is taken as the

variability of the model response and is used to calculate the percentage of discrepancy with respect to the basic simulation.

Fig. 7 shows the percentages of discrepancy for 10% variation of the chosen parameters, averaged for a whole year. The maximum percentage for any of the evaluated parameters is 4.5%. DIN and PH2 are the most sensitive variables to all the tested parameters.

In order to evaluate the sensitivity of the model to the intrinsic temporal variability of DOP and silicon, which is lost when the monthly means are calculated, we performed a two-step process. First, a weekly interpolation of both the data and their standard deviation from Loureiro et al. (2009) was performed. Second, we generated a weekly value of a normally distributed random variable a with mean of 0, and a variance and standard deviation of 1. The randomly generated number was multiplied by the weekly standard deviation of the data, and added to the weekly mean, therefore creating a new data set with which to force the model. Four runs of the *Standard simulation* (Fig. 8) and of a simulation not including the use of DOP (*No DOP Simulation*) (data not shown) were performed using different randomly generated DOP and silicon series. See section 3.4 for a description of the results.

2.5. Observational data

Weekly climatologies for temperature, salinity and chlorophyll *a* are calculated from the data collected by the Aquaculture Center of IRTA (Institute for Food and Agricultural Research and Technology) from 1990 to 2003 and published by de Pedro (2007) . Additionally, nitrate concentrations were taken from 1991 to 1994 and phosphate from 1993 to 1994de Pedro (2007). The water samples were collected weekly near the surface (0.5 m) at the center of the bay (Fig. 1). Phytoplankton data from the same sampling site (M. Delgado, unpublished data) were counted by means of the Utermöhl technique, using 50 ml sedimentation chambers and a Nikon inverted microscope. Diatoms and dinoflagellates, as well as nano and microphytoplankton from other algal groups were identified down to the lowest possible taxonomical level and enumerated. A weekly climatology is calculated for diatoms. There are not enough data to build a climatology of flagellates, since the small size and poor conservation of many of these organisms make them unsuitable for the inverted microscope technique.

The observed diatom data, given in cell numbers per unit volume, are transformed to N units for comparison purposes. We use a conversion factor of 16.2 $\pm$ 1.8 pg N cell^{-1}. This factor was calculated by (Segura-Noguera et al., Unpublished results) for diatoms from the Catalan Coast, using X ray microanalysis techniques. The values represent averages of measurements for a number of cells and can vary greatly depending on the species and on environmental characteristics. The modeled chlorophyll *a* of Fig. 5(e) was obtained by adding the N concentration of the two phytoplankton groups, using the Redfield ratio to calculate phytoplankton C and applying a C: chlorophyll ratio of 30, within the range reported by Arin et al. (2002).

Fig.3, Fig. 4 and Fig. 5 show the weekly means and the standard deviation normalized using the square root of the number of samples of these physical and biological data. A smoothing of the data was performed using the average of three consecutive averages (indicated as 3pt av in the charts).

3. Results

In order to explore all the possible scenarios regarding the use of DOP for phytoplankton growth and the addition of DIP in the water column by means of resuspension of sediments, we performed four different simulations. A first simulation incorporates both DOP use and resuspension of sediments (called *Standard Simulation* from now on). A second simulation includes DOP use but no sediment resuspension (*No Resuspension Simulation*). A third simulation comprises sediment resuspension but no DOP utilization (*No DOP Simulation*). The results for DIN, DIP, PH1 and PH2 are shown in Fig. 4 and Fig. 5. A fourth simulation with no DOP use and no resuspension (*No Extra P Simulation*) gave generally similar results to the *No DOP Simulation* (not shown but commented below).

Modeled results and available observations for dissolved inorganic nutrients (Fig. 4) and for phytoplankton and chlorophyll *a* (Fig. 5) are shown together for an easier comparison. There are no observational data for zooplankton or detritus, but the modeled results are presented in Fig. 6.

3.1. Dissolved inorganic nutrients

Measured DIN concentrations are very variable during the whole year. On average, they range between 0 and 10 mmol N m^{-3} , with occasional peaks of more than 40 mmol N m^{-3} . The general trend is a decrease in the DIN concentrations during the summer months, but the variability can be high during these months. The four simulations show two extreme patterns for DIN concentration. The *No DOP Simulation* and the *No Extra P Simulation* display similar behavior while the other two simulations present very close results. The *No DOP Simulation* (Fig. 4(b)) and the *No Extra P Simulation* (data not shown) are characterized by values of DIN that exceed 80 mmol N m^{-3} during almost one third of the year. After a minimum during February and March in which the concentrations are close to zero, DIN increases, reaches a maximum during the summer months, and decreases again from October to January. The two simulations differ only from February to April, when the *No Extra P Simulation* gives DIN values close to zero while the minimum concentrations for the *No DOP Simulation* are higher than 10 mmol N m^{-3} . These two simulations show substantial differences with the *Standard Simulation* and the *No Resuspension Simulation*, which present a DIN concentration that ranges from 0 to 20 mmol N m^{-3} between January and March, is close to zero during spring and summer, and presents some small peaks of less than 5 mmol N m^{-3} during the two last months of the year. The *Standard Simulation* and the *No Resuspension Simulation* show a similar temporal evolution to the observations.

The DIP values are low and similar in all the simulations, except for some outliers in the *Standard Simulation* and the *No DOP Simulation* that reach almost 3 mmol P m^{-3} at the beginning of February, in contrast with a maximum of 0.02 mmol P m^{-3} during the rest of the year. The measured concentrations range from 0.05 mmol P m^{-3} to 0.4 mmol P m^{-3} , although there are occasional peaks exceeding 1 mmol P m^{-3} .

3.2. Biological variables

According to the climatological data, the concentration of diatoms rises from January to October, when it reaches the maximum concentration (about 20 mmol N m^{-3} , but very variable), and decreases from October to December. Two of the four simulations show a similar general trend. In the *No Resuspension Simulation* and the *Standard Simulation* diatom biomass presents a minimum during the winter months and increases during the spring months, reaching values around 10 mmol N m^{-3} that last until December. The *No DOP Simulation* diatom biomass is, however, much lower compared to the other two simulations. Except for two peaks of 2 and 6 mmol N m^{-3} , the maximum biomass does not exceed 1 mmol N m^{-3} . There is no significant difference between the *No DOP Simulation* and the *No Extra P Simulation*.

The chlorophyll climatology displays a minimum of 2 μg l^{-1} around February and March, and a maximum in October. The simulated chlorophyll (Fig. 5(e)) for the *Standard Simulation* and the *No Resuspension Simulation* presents a similar range as the observed values, and shows a comparable seasonality, although the maximum is less marked and the minimum is too low because none of the phytoplankton groups grow when the channels are closed. The simulated chlorophyll values for *No DOP Simulation* and *No Extra P Simulation* are much lower than the measured values throughout the year.

In all simulations (Fig. 6(a)), zooplankton reaches a minimum in April. The zooplankton concentration for the period from April through December (0.4 mmol N m^{-3}) is lower for the *No DOP Simulation* than for the other two simulations (1.5 mmol N m^{-3}). The zooplankton for the *No Extra P Simulation* (results not shown) also presents a minimum in April but diverges from the *No DOP Simulation* during the first 140 days, when the concentrations are fairly stable between 0.02 and 0.06 mmol N m^{-3} .

3.3. Detritus pools

The detritus pools of both nitrogen and phosphorus follow the same pattern. The concentrations are relatively constant throughout the year, although all the simulations display a minimum at the end of March. From March to December, the detrital concentrations of the *No DOP Simulation* range between 2×10^{-3} mmol P m^{-3} and 0.03 mmol N m^{-3} and are 10 times smaller than those of the other simulations.. The DTN and DTP concentrations for the *No Extra P Simulation* (data not shown) are similar to those of the *No DOP Simulation*, with slightly lower values during the first 50 days of the year.

3.4. Sensitivity analysis

The *Standard simulation* and the *No DOP Simulation* are forced with randomly modified Si and DOP (see section 2, Materials and Methods, for details) in order to address the impact of the variability in the results. The Si changes in the *Standard Simulation* does not have any appreciable impact on the nutrients results, and the effect on the phytoplankton (Fig. 8) is within the expected variability. The Si variability does not have any effect on the *No DOP Simulation*, so the results are not shown.

The effect of the DOP on the nutrient and phytoplankton results of *Standard Simulations* is considerable. The first and last 2 months of the year are the periods that are most sensitive to the variability. More importantly, this variability may cause an increase of the DIN and a decrease of the PH1 and PH2 during November and December, which more closely resembles the climatologies of the observations.

3.5. N:P ratio

The DIN/(DIP+DOP) ratio of the *Standard Simulation* has been plotted in Fig. 9. Four more plots of the *Standard Simulation* forced with randomly generated DOP (see section 2, Materials and Methods, for details) are also shown. The *No Resuspension Simulation* gives qualitatively similar results. The dashed line is the Redfield Ratio (N/P = 16), which can be used as an orientative reference to identify of the potential limiting nutrient for phytoplankton growth. A value above the Redfield Ratio reference would indicate phosphorus limitation, while a value below the dashed line would suggest nitrogen limitation. The curve tends to be higher than the Redfiel Ratio during winter (suggesting, therefore, phosphorus limitation) and lower during summer and spring (indicative of nitrogen limitation). The nitrogen/phosphorus ratio calculated with the results of the *No Extra P Simulation* (data not shown) was always higher that 300, suggesting that in this scenario, the limiting nutrient would always be phosphorus.

4. Discussion

The ecological model presented here was designed with the aim of understanding the role played by different nutrient sources in the control of phytoplankton production in Alfacs Bay. As previously explained, our hypotheses were that there is an alternation in time between the limitation of nitrogen and phosphorus, and that, in addition to nutrient inputs from freshwater discharges and exchanges with the sea, there are two additional processes that allow this alternation: P release by sediment resuspension and the DOP source available for phytoplankton growth in addition to DIP. These hypotheses were tested by means of four simulations, including all the possible combinations of the two additional processes.

The results of the four simulations can be grouped into two categories: the simulations without use of DOP (*No DOP Simulation* and *No Extra P Simulation*) and with use of DOP (*Standard Simulation* and *No*

Resuspension Simulation). In the first set of simulations, the DIN concentration during the summer months reaches values that do not behave like the observations. Similarly, diatom abundance and chlorophyll *a* deviate largely from the climatological observations. The second set of simulations leads to results that agree with the temporal evolution of the nutrients, chlorophyll *a* and phytoplankton abundance. There are no data in Alfacs to compare with ZOO, but the modeled ZOO ranges for the simulations that include DOP are similar to measured values in the Mediterranean coastal areas (Calbet et al., 2001).

The forcing of Si and DOP in the model is done by means of a monthly climatology published by Loureiro et al. (2009). However, the concentration of DOP is, in fact, highly variable, as indicated by the high standard deviation associated with the monthly means (Fig. 3). As can be seen in the simulations of Fig. 8, variability in DOP translates into appreciable changes of variables such as DIN and chlorophyll, but all simulations present the same seasonality pattern.

Based upon the model simulations, we showed that there must be an extra source of phosphorus essential for the development of the planktonic community other than the DIP from fresh and marine waters. It is clearly shown in the results of the *No Extra P Simulation*, that without that extra source of phosphorus the organisms are phosphorus limited and are not capable of using the DIN. As a consequence, the DIN is too high, and the PH1 and chlorophyll are too low.

The idea that resuspension of sediments plays an important role in the ecosystem response appears to be somewhat inaccurate. The resuspension mechanism introduces phosphorus into the water column, but the amount of phosphorus in the mixed layer from this resuspension is low compared with the other DIP sources. It is, therefore, not possible to explain the magnitude of observed variables by only taking into account the resuspension mechanism, and it is not possible to differentiate significantly between a simulation that includes resuspension and a simulation that does not. We recognize that there are periods during which the concentrations of the mixed layer are most sensitive to the resuspension of sediment. These are the periods of closed channels, with lower DIN inflow. A small addition of phosphorus could induce a switch in the nutrient limitation. During these months, the wind is stronger than in summer and the lack of freshwater discharge from the channels weakens the stratification, making it easier to generate sediment resuspension. The results of the model show that the closed channel period is the only period where the *No Extra P Simulation* and the *No DOP Simulation* differ, with higher PH1 and PH2 concentrations in the *No DOP Simulation*. Thus, we cannot discard the possibility that resuspension has a relatively minor role during the closed channel months. In addition, there might be episodic events when particularly strong resuspension of sediments can bring larger amount of phosphorus to the water column.

Sediment resuspension in Alfacs Bay (Guillén, 1992) has two origins, i.e. by currents coming from the south and entering the bay through the mouth, and wind stirring. As we lack field data from currents

and it appears that events of sediment resuspension by currents are less common than by wind stirring, the model considered only this last mechanism. This does not exclude the fact that sediment resuspension could be more important during periods of high currents. While the influence of sediment resuspension on DIP concentrations of the mixed layer was found to be negligible, it is also possible that the resuspension mechanism could affect the DIP concentration of the deep layer and its nitrogen cycle. Finally, the load of phosphorus from sediments could be affected by episodes of anoxia, because the phosphorus is liberated in soluble form in anoxic environments (Golterman, 2001). Anoxia, however, rarely occurs in Alfacs Bay (Camp et al., 1991; de Pedro, 2007).

Availability of the extra source of phosphorus, Dissolved Organic Phosphorus, and its utilization by phytoplankton play an important role in the dynamics of the ecosystem in Alfacs Bay. They alleviate phosphorus stress or limitation and enable the organisms to take up more DIN and grow to ranges consistent with observations. The model shows evidence that Dissolved Organic Phosphorus utilization is indeed a key process that explains the observed magnitudes of DIN and chlorophyll *a* in Alfacs Bay.

Loureiro et al. (2009) have associated DOP inputs in Alfacs Bay with freshwater discharges. The concentrations of DOP range from 0 to 1.2 mmol m^{-3}, but its origin is not well known. Forès (1989) and Forès (1992), in an study related to the nutrient fluxes in rice fields in the Ebre Delta, observed a release of DOP during several phases of rice growth lasting about 115 days, from April to mid July. The measured DOP in Alfacs peaks between the end of July and the beginning of August, suggesting that during the first months (April to June) most of the DOP comes from the rice fields through discharge channels. During the last months (July to November), it is probably released from organisms or from detrital organic matter.

Finally, we explored the question of nitrogen and phosphorus limitation of phytoplankton growth and the role of these nutrients on the phytoplankton species composition during different seasons. The alternation between phosphorus and nitrogen limitation can be observed in Fig. 8. The periods of high nitrogen concentration at the beginning and, to a lesser extent, the end of the year, coincide with periods of low phosphorus, while the highest availability of phosphorus, due to DOP, which tends to occur between May and October, coincides with low DIP limitation. A similar seasonality pattern was observed by (Fisher et al., 1992), who related it to changes in the composition of freshwater inputs. A comparison of Figs. 3(h) and 9, suggests that the main drivers of the changes in nitrogen and phosphorus availability are the freshwater fluxes from the channels and the DOP inputs.

In order to describe in more detail the alternation of nutrient limitation observed in the simulations that include DOP, the DIN/(DIP+DOP) ratio of the *Standard Simulation* and the DIN/(DIP+DOP) ratio for four *Standard Simulations* forced with randomly modified DOP is shown in Fig. 9. The observed pattern suggests a potential phosphorus limitation during winter while, during summer and spring, when DOP tends to be

higher, the limitation is more likely to be due to nitrogen. In fall the limitation switches from nitrogen to phosphorus depending on the availability of DOP.

In accordance with observations in other estuaries, the switch in limiting nutrients over the year has an effect on phytoplankton biomass, composition and seasonal cycle (D'Elia et al., 1986; Fisher et al., 1992; McComb and Others, 1981). N and P availability in general could also influence the biochemical composition of phytoplankton and could be important in relationship with food quality for zooplankton and for the other components of the trophic network (Estrada et al., 2008). From a management point of view, the alternation of phosphate and nitrogen limitation suggests the need to control the inputs of both nutrients in order to avoid potential eutrophication problems.

The role of DOP availability on the phytoplanktonic community must be recognized as important in Alfacs Bay. It has been shown that phytoplankton species differ in their ability to utilize DOP. In particular, it has been shown that some HAB-forming dinoflagellates like *Alexandrium tamarense* or *Prorocentrum minimum* (which are present in Alfacs) grow well on DOP. This ability could help them to outcompete other species and cause noxious outbreaks, particularly in situations of DIP depletion (Heil et al., 2005; Oh et al., 2002).

While our model study points towards the important role of DOP in the Bay, we have to mention that our model did not take into account the possible contribution of dissolved organic nitrogen (DON) to phytoplankton growth (Berman and Bronk, 2003). This ability could favor some taxa, as suggested by Loureiro et al. (2009) to explain *Pseudo-nitzschia* spp. dynamics. However, the relatively low concentrations of DON, which does not exceed 12 mmol m^{-3} in May to October, in relation to the high DIN inputs suggest that DON contributions would not modify the overall conclusions regarding nutrient limitation. We also need to gain insight into allochthonous sources of DOP and into its metabolism in the planktonic community. Future models should include DOP as a state variable.

The results of our modelling study also highlight some key aspects that need to be addressed in future studies in order to improve our understanding of the nutrient budgets and the ecosystem processes in Alfacs Bay.

Given the importance of the freshwater discharges as evidenced in this study, we find it necessary to have long time series of flows and nutrient content of freshwaters entering the bay, both from the drainage channels and from ground water discharges. According to Llebot (2007), who used a 3D free-surface hydrostatic model of water circulation in Alfacs Bay, the existence of substantial underground water inputs was essential to explain the water column structure observed in winter. Given the potentially high nutrient concentrations in these waters it is important to better constrain their fluxes and composition.

The 0–dimensional model presented here has been useful to test our hypotheses. However, it has been

shown that there is a north to south gradient of the ecological dynamics caused by the presence of freshwater discharges in the north shore (Delgado and Camp, 1987). Spatial heterogeneities have been observed in the sediment and, therefore, in the nutrient flow from the sediment Vidal et al. (1992). These heterogeneities, combined with certain recirculation patterns, could favor the proliferation of certain species or groups of species. Three-dimensional simulations would allow a more detailed analysis of the spatio-temporal variability of the studied ecosystem.

5. Conclusions

We have used a simple ecological model to extract important conclusions about the nutrient budget in a Mediterranean estuarine bay. Based on the simulation of four scenarios for Alfacs Bay involving the presence or absence of DOP use by phytoplankton, and the presence or absence of DIP inputs from sediment resuspension, we suggest that DOP plays a key role in providing a phosphorus source that allows build-up of phytoplankton biomass and nitrate draw-down. Sediment resuspension does not appear to be a significant source of phosphorus, although it could have some effect during the periods of low nitrogen load. The inclusion of DOP as a phosphorus source leads to an alternation between phosphorus (winter) and nitrogen (spring and summer) limitation. The limitation during fall switches from nitrogen to phosphorus depending on the amount of DOP.

References

Arin, L., Anxelu, X., Moran, G., Estrada, M., 2002. Phytoplankton size distribution and growth rates in the Alboran Sea (SW Mediterranean): short term variability related to mesoscale hydrodynamics. J. Plankton. Res. 24 (10), 1019–1033.

Artigas, M. L., 2008. Estudi de la comunitat fitoplanctònica en relació amb la hidrodinàmica de la columna d'aigua a la badia dels Alfacs (NO Mediterrani). Master's thesis, Universitat de Barcelona.

Bentzen, E., Taylor, W. D., Millard, E. S., 1992. The importance of dissolved organic phosphorus to phosphorus uptake by limnetic plankton. Limnol. Oceanogr. 37 (2), 217–231.

Berman, T., Bronk, D. A., 2003. Dissolved organic nitrogen: a dynamic participant in aquatic ecosystems. Aquat. Microb. Ecol. 31, 279–305.

Boyle, D. R., 1994. Design of a seepage meter for measuring groundwater fluxes in the nonlittoral zones of lakes – evaluation in a boreal forest lake. Limnol. Oceanogr. 39 (3), 670–681.

Brainerd, K. E., Cregg, M. C., 1995. Surface mixed and mixing layer depths. DSR 42 (9), 1521–1543.

Calbet, A., Garrido, S., Saiz, E., Alcaraz, M., Duarte, C. M., 2001. Annual zooplankton succession in coastal NP Mediterranean waters: the importance of the smaller size fractions. J. Plankton. Res. 23 (3), 319–331.

Camp, J., 1994. Aproximaciones a la dinámica ecológica de una bahía estuárica mediterránea. Ph.D. thesis, Universitat de Barcelona.

Camp, J., Delgado, M., September 1987. Hidrografía de las bahías del delta del ebro. Inv.Pesq. 51 (3), 351–369.

Camp, J., Romero, J., Pérez, M., Vidal, M., Delgado, M., Martínez, A., 1991. Production – consumption budget in an estuarine bay: how anoxia is prevented in a forced system. Oceologia aquatica 10, 145–152.

Chapelle, A., Ménesguen, A., Deslous-Paoli, J.-M., Souchu, P., Mazouni, N., Vaquer, A., Millet, B., 2000. Modelling nitrogen, primary production and oxygen in a mediterranean lagoon. impact of oysters farming and inputs from the watershed. Ecol. Model. 127, 161–181.

Chen, C., Ji, R., Schwab, D. J., Beletsky, D., Fahnenstiel, G. L., Jiang, M., Johengen, T. H., Vanderploeg, H., Eadie, B., Budd, J. W., Bundy, M. H., Gardner, W., Cotner, J., Lavrentyev, P. J., 2002. A model study of the coupled biological and physical dynamics in lake michigan. Ecol. Model. 152, 145–168.

Crispi, G., Crise, A., Solidoro, C., 2002. Coupled mediterranean ecomodel of the phosphorus and nitrogen cycles. J. Marine Sys. 33–34, 497–521.

Cruzado, A., Velásquez, Z., del Carmen Pérez, M., Bahamón, N., Grimaldo, N. S., Ridolfi, F., 2002. Nutrient fluxes from the ebro river and subsequent across-shelf dispersion. Cont. Shelf Res. 22, 349–360.

Currie, D. J., Kalff, J., 1984. A comparison of the abilities of freshwater algae and bacteria to acquire and retain phosphorus. Limnol. Oceanogr. 29 (2), 298–310.

DAAAR, 2008. Estadística de producció d'aqüicultura 2008. Departament d'Agricultura, Alimentació i Acció Rural, Generalitat de Catalunya.
URL `http://www20.gencat.cat/docs/DAR/PE_Pesca_aquicultura/PE01_Aquicultura/Documents/Fitxers_estatics/2008_estadistica_produccio_aquicultura.pdf`

de Pedro, X., 2007. Anoxic situations in estuarine zones without tidal forcing. an approach to the oxygen production/consumption budgets. Ph.D. thesis, Ecology department, University of Barcelona, Barcelona.

Delgado, M., Camp, J., September 1987. Abundancia y distribución de nutrientes orgánicos disueltos en las bahías del delta del Ebro. Inv.Pesq. 51 (3), 527–441.

Delgado, M., Estrada, M., Camp, J., Fernández, J. V., Santmartí, M., Lletí, C., March 1990. Development of a toxic *Alexandrium minutum* Halim (Dinophyceae) bloom in the harbour of Sant Carles de la Ràpita (Ebro Delta, Northwestern Mediterranean). Sci. Mar. 54 (1), 1–7.

D'Elia, C. F., Sanders, J. G., Boynton, W. R., 1986. Nutrient enrichment studies in a coastal plain estuary: phytoplankton growth in large-scale continuous cultures. Can. J. Fisheries Aquat. Sci. 43, 397–406.

Estrada, M., Sala, M. M., van Lenning, K., Alcaraz, M., Felipe, J., Veldhuis, M. J. W., 2008. Biological interactions in enclosed plankton communities including *Alexandrium catenella* and copepods: Role of phosphorus. J. Exp. Mar. Biol. Ecol. 355, 1–11.

Farnós, A., Ribas, X., Reverté, J. T., June 2007. El Canal Porta Vida. Exhibition, Museu Comarcal del Montsià.
URL `http://www.diputaciodetarragona.cat/houdipu/media/upload/pdf/expo_canal_porta_vida_ed265bc903a5a097f61d3ec064d96d2e345.pdf`

Fasham, M., 1995. Variations in the seasonal cycle of biological production in subarctic oceans: A model sensitivity analysis. Deep-Sea Res. 42, 1111–1149.

Fasham, M. J. R., Ducklow, H. W., McKelvie, S. M., 1990. A nitrogen-based model of plankton dynamics in the oceanic mixed layer. J. Mar. Res. 48, 591–639.

Fennel, K., Spitz, Y., Letelier, R. M., Abbott, M. R., Karl, D. M., 2002. A deterministic model for N_2 Fixation at stn. ALOHA in the subtropical North Pacific Ocean. DSR2 49, 149–174.

Fennel, W., Neumann, T., 2004. Introduction to the modelling of marine ecosystems, illustrated Edition. Elsevier.

Fernández-Tejedor, M., Soubrier-Pedreño, M. A., Furones, M. D., 2004. Acute LD_{50} of a *Gyrodinium corsicum* natural population for *Sparus aurata* and *Dicentratchus labrax*. Harmful Algae 3, 1–9.

Fisher, H. B., List, E. J., Koh, R. C. Y., Imberger, J., Brooks, N. H., 1979. Mixing in inland and coastal waters. Academic Press.

Fisher, T. R., Peele, E. R., Ammerman, J. W., Harding, L. W., 1992. Nutrient limitation of phytoplankton in Chesapeake Bay. Mar. Ecol. Progr. Ser. 82, 51–63.

Forès, E., 1989. Ricefields as filters. Arch. Hydrobiol 116 (4), 517–527.

Forès, E., 1992. Nutrient loading and drainage channel response in a ricefield system. Hydrobiol. 230, 193–200.

Forès, E., Comín, F. A., 1992. Ricefields, a limnological perspective. Limnetica 10, 101–109.

Franks, P. J. S., 2002. NPZ models of plankton dynamics: their construction, coupling to physiscs and application. J. Oceanogr. 58, 379–378.

Froelich, P. N., 1988. Kinetic control of dissolved phosphate in natural rivers and estuaries. Limnol. Oceanogr. 33 (4, part 2), 649–668.

Garcés, E., Delgado, M., Camp, J., 1997. Phased cell division in a natural population of *Dinophysis sacculus* and the *in situ* measurement of potential growth rate. J. Plankton. Res. 19 (12), 2067–2077.

Garcés, E., Delgado, M., Masó, M., Camp, J., 1999. *In situ* growth rate and distribution of the ichthyotoxic dinoflagellate *Gyrodinium corsicum* paulmier in an estuarine embayment (Alfacs Bay, NW Mediterranean Sea). J. Plankton. Res. 21 (10), 1977–1991.

Giraud, X., 2006. Modelling an alkenone-like proxy record in the nw african upwelling. Biogeosciences 3, 251–269.

Golterman, H. L., 2001. Phosphate release from anoxic sediments or 'what did mortimer really write?'. Hydrobiol. 450, 99–106.

Guillén, J., 1992. Dinámica y balance sedimentario en los ambientes fluvial y litoral del Delta del Ebro. Ph.D. thesis, Universitat Politècnica de Catalunya.

Hamby, D. M., 1994. A review of techniques for parameter sensitivity analysis of environmental models. Environ. Monit. Assess. 32, 135–154.

Heil, C. A., Glibert, P. M., Fan, C., 2005. *Prorocentrum minimum* (pavillard) schiller a review of a harmful algal bloom species of growing worldwide importance. Harmful Algae 4, 449–470.

Howarth, R. W., Marino, R., 2006. Nitrogen as the limiting nutrient for eutrophication in coastal marine ecosystems: evolving views over three decades. Limnol. Oceanogr. 51 (1, part 2), 364–376.

Huang, B., Hong, H., 1999. Alkaline phosphatase activity and utilization of dissolved organic phosphorus by algae in subtropical coastal waters. Mar. Pollut. Bull. 39 (1–12), 205–211.

Jassby, A. D., Platt, T., 1976. Mathematical formulation of the relationship between photosynthesis and light for phytoplankton. Limnol. Oceanogr. 21, 540–547.

Johannes, R. E., 1964. Uptake and release of dissolved organic phosphorus by representatves of a coastal marine ecosystems. Limnol. Oceanogr. 9 (2), 224–234.

Kishi, M. J., Kashiwai, M., Ware, D. M., Megrey, B. A., Eslinger, D. L., Werner, F. E., Noguchi-Aita, M., Azumaya, T., Fujii, M., Hashimoto, S., Huang, D., Iizumi, H., Ishida, Y., Kang, S., Kantakov, G. A., cheol Kim, H., Komatsu, K., Navrotsky, V. V., Smith, S. L., Tadokoro, K., Tsuda, A., Yamamura, O., Yamanaka, Y., Yokouchi, K., Yoshie, N., Zuenko, J. Z. Y. I., Zvalinsky, V. I., 2007. NEMURO – a lower trophic level model for the North Pacific marine ecosystem. Ecol. Model. 202, 12–25.

Lacroix, G., Nival, P., 1998. Influence of meteorological variabilitu on primary production dynamics in the Ligurian Sea (NW Mediterranean Sea) with a 1D hydrodynamic/biological model. J. Marine Sys. 16, 23–50.

Lancelot, C., Spitz, Y., Gypens, N., Ruddick, K., Becquevort, S., Rousseau, V., Lacroix, G., Billen, G., 2005. Modelling diatom and *Phaeocystis* blooms and nutrient cycles in the southern bight of the north sea: the miro model. Mar. Ecol. Progr. Ser. 289, 63–78.

le Quéré, C., Harrison, S. P., Prentice, I. C., Buitenhuis, E. T., Aumont, O., Bopp, L., Claustre, H., Cunha, L. C. D., Geider, R., Giraud, X., Klaas, C., Kohfeld, K. E., Legendre, L., Manizza, M., Platt, T., Rivkin, R. B., Sathyendranath, S., Uitz, J., Watson, A., Wolf-Gladrow, D., 2005. Ecosystem dynamics based on plankton functional types for global ocean biogeochemistry. Glob. Change Biol. 11, 2016–2040.

Lebo, M. E., 1991. Particle–bound phosphorus along an urbanized coastal plain estuary. Mar. Chem. 34, 225–246.

Lima, I. D., Olson, D. B., Doney, S. C., 2002. Intrinsic dynamics and stability properties of size-structured pelagic ecosystem models. J. Plankton. Res. 24 (6), 533–556.

Llebot, C., November 2007. Hydrodynamic characterization of a Mediterranean bay using Si3D, a three–dimensional model for estuarine circulation. Master's thesis, Universidad de las Palmas de Gran Canaria.

Llebot, C., Delgado, M., Turiel, A., Fernández-Tejedor, M., Diogène, J., Camp, J., Solé, J., Estrada, M., 2008. Coupling phytoplankton

and hydrography in alfacs bay using principal component analysis and empirical mode decomposition. In: European Geosciences Union. General Assembly 2008. Poster.

Loureiro, S., Garcés, E., Fernández-Tejedor, M., Vaqué, D., Camp, J., 2009. *Pseudo-nitzschia* spp. (Bacillariophyceae) and dissolved organic matter (DOM) dynamics in the Ebro Delta (Alfacs Bay, NW Mediterranean Sea). Estuar. Coast. Shelf Sci. 83, 539–549.

Malone, T. C., Conley, D. J., Fisher, T. R., Glibert, P. M., Harding, L. W., Sellner, K. G., 1996. Scales of nutrient–limited phytoplankton productivity in chesapeake bay. Estuaries 19 (2B), 371–385.

McComb, A. J., Others, 1981. Eutrophication in the peel-harvey estuarine system, western australia. In: Neilson, B. J., Cronin, L. E. (Eds.), Estuaries and nutrients. N. J. Cifton and Humana Press, pp. 323–342.

Merico, A., Tyrrell, T., Lessard, E. J., Oguz, T., Stabeno, P. J., Zeeman, S. I., Whitledge, T. E., 2004. Modelling phytoplankton succession on the Bering Sea shelf: role of climate influences and trophic interactions in generating *Emiliana huxleyi* blooms 1997-2000. DSR 51, 1803–1826.

Ministerio de Obras Públicas, Transportes y Medio Ambiente; Ministerio de Industria y Energía, 1995. Libro blanco de las aguas subterráneas.

Muñoz, I., 1998. Carbono, nitrógeno y fósforo en la parte baja del río Ebro y en los canales de riego del Delta. Oceologia aquatica 11, 23–25.

Oh, S. J., Yamamoto, T., Kataoka, Y., Matsuda, O., Matsuyama, Y., Kotani, Y., May 2002. Utilization of dissolved organic phosphorus by the two toxic dinoflagellates *Alexandrium tamarense* and *Gymnodinium catenatum* (dinophyceae). Fish. Sci. 68 (2), 416–424.

O'Neill, R. V., DeAngelis, D. L., Pastor, J. J., Jackson, B. J., Post, W. M., 1989. Multimple nutrient limitations in ecological models. Ecol. Model. 46, 174–163.

Platt, T., Callegos, C. L., Harrison, W. G., 1980. Photoinhibition of photosynthesis in natural assemblages of marine phytoplankton. J. Mar. Res. 38 (4), 687–701.

Quijano-Sheggia, S., Garcés, E., Flo, E., Fernández-Tejedor, M., Diogène, J., Camp, J., 2008. Bloom dynamics of the genus *Pseudo nitzschia* (Bacillariophyceae) in two coastal bays (NW Mediterranean Sea). Sci. Mar. 72 (3), 577–590.

Salat, J., Garcia, M. A., Cruzado, A., Palanques, A., Arin, L., Gomis, D., Guillén, J., de León, A., Puigdefàbregas, J., Sospedra, J., Velásquez, Z. R., 2002. Seasonal changes of water mass structure and shelf slope exchanges at the Ebro Shelf (NW Mediteranean). Cont. Shelf Res. 22, 327–348.

Segura-Noguera, M., Fortuño, J. M., Blasco, D., Unpublished results. Elemental composition of individual dinoflagellate and diatom cells from the Catalan Sea (NW Mediterranean Sea), unpublished results.

Smith, C. G., Cable, J. E., Martin, J. B., , M. R., 2008. Evaluating the source and seasonality of submarine groundwater discharge using a radon-222 pore water transport model. Earth Planet. Sci. Lett. 273, 312–322.

Smith, E. L., 1936. Photosynthesis in relation to light and carbon dioxide. Proc. Natl. Acad. Sci 22, 504–511.

Solé, J., Turiel, A., Estrada, M., Llebot, C., Blasco, D., Camp, J., Delgado, M., Fernández-Tejedor, M., Diogène, J., 2009. Climatic forcing on hydrography of a mediterranean bay (alfacs bay). Cont. Shelf Res. In Press, Accepted Manuscript, –.

Spitz, Y. H., Moisan, J. R., Abbott, M., 2001. Configuring an ecsystem model using data from the Bermuda Atlantic Time Series (BATS). DSR2 48, 1733–1768.

Stalker, J. C., Price, R. M., Swart, P. K., 2009. Determining spatial and temporal inputs of freshwater, including submarine groundwater discharge, to a subtropical estuary using geochemical tracers, biscayne bay, south florida. Estuaries Coasts 32, 694–708.

Taft, J. L., Taylor, W. R., McCarthy, J. J., 1975. Uptke and release pf phosphorus by phytoplankton in the Chesapeake Bay Estuary, USA. Marine Biol. 33, 21–32.

Torrecilla, N. J., Galve, J. P., Zaera, L. G., Retamar, J. F., Álvarez, A. N., 2005. Nutrient sources and dynamics in a mediterranean fluvial regime (ebro river, ne spain) and their implications for water management. J. Hydrol. 304, 166–182.

Tyrrell, T., August 1999. The relative influences of nitrogen and phosphorus on oceanic primary production. Nature 400, 525–531.

van den Berg, A. J., Ridderinkhof, H., Riegman, R., Ruardij, P., Lenhart, H., 1995. Influence of variability in water transport on

phytoplankton biomass and composition in the southern North Sea: a modelling apporach (FYFY). Cont. Shelf Res. 16 (7), 907–931.

Vidal, M., July 1994. Phosphate dynamics tied to sediment disturbances in Alfacs Bay (NW Mediterranean). Mar. Ecol. Prog. Ser. 110, 211–221.

Vidal, M., Morguí, J., Latasa, M., Romero, J., Camp, J., 1992. Factors controlling spatial variability in ammonium release within an estuarine bay (Alfacs Bay, Ebro Delta,NW Mediterranean). Hydrobiol. 235/236, 519–525.

Vila, M., Garcés, E., Masó, M., , Camp, J., 2001. Is the distribution of the toxic dinoflagellate *Alexandrium catenella* expanding along the NW Mediterranean coast? Mar. Ecol. Progr. Ser. 222, 73–83.

Yamamoto, T., Oh, S. J., Kataoka, Y., 2004. Growth and uptake kinetics for nitrate, ammonium and phosphate by the toxic dinoflagellate *Gymnodinium catenatum* isolated from Hiroshima Bay, Japan. Fish. Sci. 70, 108–115.

6. Acknowledgements

This work was funded by projects TURECOTOX (CTM2006-13884-CO2-00/MAR9, Ministerio of Ciencia e Innovación, Spain) and CANESP (a joint project between the National Research Council of Canada and the Ministerio de Asuntos Exteriores of Spain), and by the CSIC. CL was supported by a fellowship of the Spanish National Research Council, CSIC (Beca CSIC Predoctoral I3P-BPD2005). The modeling was performed during CL's internship in the College of Oceanic and Atmospheric Sciences at Oregon State. We thank Tim Cowles for hosting CL during her first stay in the US and for his help and support during the first stages of the model development. JS was funded by Proyecto Intramural Especial del CSIC, 'Desarrollo de algoritmos y validación de productos en el Centro Experto SMOS en Barcelona' (200430E530). We are grateful to Maximinio Delgado for kindly providing phytoplankton data and to Elisa Berdalet, Esther Garcés and Mariona Segura for valuable advice and information. Aquaculture Center of IRTA (Institut de Recerca i Tecnologia Agroalimentàries, Generalitat de Catalunya) sponsored the collection of time series of environmental data in Alfacs Bay. The Servei Meteorològic de Catalunya and the Instituto Nacional de Meteorología provided meteorological data.

$$\frac{\partial \mathrm{PH1}}{\partial t} = \mathrm{Growth}_{(\mathrm{PH1})}\ \mathrm{PH1} - \mathrm{Death}_{(\mathrm{PH1})}\ \mathrm{PH1} - \mathrm{Grazing}_{(\mathrm{PH1})}\ \mathrm{ZOO} + \mathrm{Advection}_{(\mathrm{PH1})} \tag{2}$$

$$\frac{\partial \mathrm{PH2}}{\partial t} = \mathrm{Growth}_{(\mathrm{PH2})}\ \mathrm{PH2} - \mathrm{Death}_{(\mathrm{PH2})}\ \mathrm{PH2} - \mathrm{Grazing}_{(\mathrm{PH2})}\ \mathrm{ZOO} + \mathrm{Advection}_{(\mathrm{PH2})} \tag{3}$$

$$\frac{\partial \mathrm{ZOO}}{\partial t} = \gamma\ (\mathrm{Grazing}_{(\mathrm{PH2})} + \mathrm{Grazing}_{(\mathrm{PH1})})\ \mathrm{ZOO} - \mathrm{Death}_{(\mathrm{ZOO})}\ \mathrm{ZOO}^2 - \mathrm{Excretion}_{(\mathrm{ZOO})}\ \mathrm{ZOO} + \mathrm{Advection}_{(\mathrm{ZOO})} \tag{4}$$

$$\frac{\partial \mathrm{DIN}}{\partial t} = -\mathrm{Growth}_{(\mathrm{PH2})}\ \mathrm{PH2} - \mathrm{Growth}_{(\mathrm{PH1})}\ \mathrm{PH1} + \mathrm{Excretion}_{(\mathrm{ZOO})}\ \mathrm{ZOO} + \mathrm{Remineralisation}_{(\mathrm{DTN})}\ \mathrm{DTN} + \mathrm{FWInput}_{(\mathrm{DIN})} + \mathrm{Advection}_{(\mathrm{DIN})} \tag{5}$$

$$\frac{\partial \mathrm{DIP}}{\partial t} = \mathrm{NPRedfield} \times \Big(- \mathrm{Growth\_eq}_{(\mathrm{PH2})}\ \mathrm{PH2} - \mathrm{Growth\_eq}_{(\mathrm{PH1})}\ \mathrm{PH1} + \mathrm{Excretion}_{(\mathrm{ZOO})}\ \mathrm{ZOO}\Big) + \mathrm{Remineralisation}_{(\mathrm{DTP})}\ \mathrm{DTP} + \mathrm{FWInput}_{(\mathrm{DIP})} + \mathrm{Resuspension}_{(\mathrm{DIP})} + \mathrm{Advection}_{(\mathrm{DIP})} \tag{6}$$

$$\frac{\partial \mathrm{DTN}}{\partial t} = (1-\gamma)(\mathrm{Grazing}_{(\mathrm{PH2})} + \mathrm{Grazing}_{(\mathrm{PH1})})\ \mathrm{ZOO} + \mathrm{Death}_{(\mathrm{PH2})}\ \mathrm{PH2} + \mathrm{Death}_{(\mathrm{PH1})}\ \mathrm{PH1} + \mathrm{Death}_{(\mathrm{ZOO})}\ \mathrm{ZOO}^2 - \mathrm{Remineralisation}_{(\mathrm{DTN})}\ \mathrm{DTN} + \mathrm{Sedimentation}_{(\mathrm{DTN})} + \mathrm{Advection}_{(\mathrm{DIN})} \tag{7}$$

$$\frac{\partial \mathrm{DTP}}{\partial t} = \mathrm{NPRedfield} \times \Big((1-\gamma) \times (\mathrm{Grazing}_{(\mathrm{PH2})} + \mathrm{Grazing}_{(\mathrm{PH1})})\ \mathrm{ZOO} + \mathrm{Death}_{(\mathrm{PH2})}\ \mathrm{PH2} + \mathrm{Death}_{(\mathrm{PH1})}\ \mathrm{PH1} - \mathrm{Death}_{(\mathrm{ZOO})}\ \mathrm{ZOO}^2\Big) - \mathrm{Remineralisation}_{(\mathrm{DTP})}\ \mathrm{DTP} + \mathrm{Sedimentation}_{(\mathrm{DTP})} + \mathrm{Advection}_{(\mathrm{DIN})} \tag{8}$$

Table 1: Governing equations.

Symbol	Value	Units	Description
Basic parameters of the model			
dt	15	min	Time step
Basic parameters of the plankton			
$P^B_{m(\mathrm{PH1})}$	2.75	day^{-1}	Maximum diatom growth rate
$P^B_{m(\mathrm{PH2})}$	2.25	day^{-1}	Maximum flagellate growth rate
$Kp_{(\mathrm{PH1})}$	1.0	mmol N m^{-3}	Diatom half saturation constant for ingestion
$Kp_{(\mathrm{PH2})}$	1.0	mmol N m^{-3}	Flagellate half saturation constant for ingestion
$m_{(\mathrm{PH1})}$	0.08	day^{-1}	Diatoms mortality rate
$m_{(\mathrm{PH2})}$	0.08	day^{-1}	Flagellates mortality rate
$m_{(\mathrm{ZOO})}$	0.15	day^{-1}	Zooplankton mortality rate
R_m	1.	day^{-1}	Zooplankton maximum grazing rate
$\chi_{(\mathrm{PH1})}$	0.3	No dim	Preference of zooplankton for grazing on diatom
$\chi_{(\mathrm{PH2})}$	0.7	No dim	Preference of zooplankton for grazing on flagellate
E	0.03	day^{-1}	Zooplankton excretion rate
$NPRedfield$	1/16	No dim	Redfield ratio
Basic parameters of the bay			
A	49000000	m^2	Area
ML	2500	m^2	Mouth length
φ	40.5	$^\circ$N	Latitude
Light limitation			
PAR	0.48	%	Photosinthetically active radiation
I_0	340	W m^{-2}	Incoming solar radiation
θ	0.04	No dim	Albedo
$\alpha_{(\mathrm{PHX})}$	0.07	mmolN h^{-1} W^{-1} m^{-2}	Slope of the light saturation curve
Colimitation of nutrients			
$K_{\mathrm{DIN,PH1}}$	0.5	mmol N m^{-3}	DIN half saturation constant for diatoms
$K_{\mathrm{P,PH1}}$	0.045	mmol P m^{-3}	P half saturation constant for diatoms
$K_{\mathrm{Si,PH1}}$	5	mmol Si m^{-3}	Si half saturation constant for diatoms
$K_{\mathrm{DIN,PH2}}$	0.4	mmol N m^{-3}	DIN half saturation constant for flagellates
$K_{\mathrm{P,PH2}}$	0.04	mmol P m^{-3}	P half saturation constant for flagellates
Sedimentation			
$\phi_{(\mathrm{DTN})}$	8	m s^{-1}	Sinking velocity of DTN
$\phi_{(\mathrm{DTP})}$	8	m s^{-1}	Sinking velocity of DTP
Mixed layer depth			
L	11000	m	Length scale of the bay
g	9.81	m s^{-2}	Acceleration of gravity
C_D	1.3 $\times 10^{-3}$	No dim	Drag coefficient
ρ_a	1.2	kg m^{-3}	Air density
Inputs of freshwater			
$\mathrm{C}_{(dis,\mathrm{DIN})}$	70	mmol N m^{-3}	Concentration of DIN in discharge channels
$\mathrm{C}_{(dis,\mathrm{DIP})}$	0.5	mmol N m^{-3}	Concentration of DIP in discharge channels
$\mathrm{C}_{(und,\mathrm{DIN})}$	500	mmol N m^{-3}	concentration of DIN in underground water
$\mathrm{C}_{(und,\mathrm{DIP})}$	0.5	mmol N m^{-3}	Concentration of DIP in underground water
F_{und}	120960	m^3 day^{-1}	Minimum underground water flow
Resuspension of sediments			
$Pflow$	65	mmol m^{-3} m^{-2} h^{-1}	Mean DIP flow for the first 30 min after the sediment resuspension.
Peq	0.2	mmol m^{-3}	Equilibrium concentration of DIP after 30 minutes from the sediment resuspension
Advection			
$\mathrm{Ocean}_{(\mathrm{PH1})}$	0	mmol m^{-3}	Ocean concentration of diatoms
$\mathrm{Ocean}_{(\mathrm{PH2})}$	0	mmol m^{-3}	Ocean concentration of flagellates

Table 2: Parameters. Continues in next page.

Symbol	Value	Units	Description
$\text{Ocean}_{(\text{ZOO})}$	0	mmol m^{-3}	Ocean concentration of zooplankton
$\text{Ocean}_{(\text{DIN})}$	1	mmol m^{-3}	Ocean concentration of dissolved inorganic nitrogen
$\text{Ocean}_{(\text{DIP})}$	0.05	mmol m^{-3}	Ocean concentration of dissolved inorganic phosphorus
$\text{Ocean}_{(\text{DTN})}$	0	mmol m^{-3}	Ocean concentration of detrital nitrogen
$\text{Ocean}_{(\text{DTP})}$	0	mmol m^{-3}	Ocean concentration of detrital phosphorus
$\text{OceanW}_{(\text{PH1})}$	0	mmol m^{-3}	Ocean concentration of diatoms in winter
$\text{OceanW}_{(\text{PH2})}$	0	mmol m^{-3}	Ocean concentration of flagellates in winter
$\text{OceanW}_{(\text{ZOO})}$	0	mmol m^{-3}	Ocean concentration of zooplankton in winter
$\text{OceanW}_{(\text{DIN})}$	3	mmol m^{-3}	Ocean concentration of dissolved inorganic nitrogen in winter
$\text{OceanW}_{(\text{DIP})}$	0.15	mmol m^{-3}	Ocean concentration of dissolved inorganic phosphorus in winter
$\text{OceanW}_{(\text{DTN})}$	0	mmol m^{-3}	Ocean concentration of detrital nitrogen in winter
$\text{OceanW}_{(\text{DTP})}$	0	mmol m^{-3}	Ocean concentration of detrital phosphorus in winter
Remineralisation			
D_{DTN}	0.1	day$^{-}1$	Detritic nitrogen remineralisation rate
D_{DTP}	0.2	day$^{-}1$	Detritic phosphorus remineralisation rate
DOP			
$Ks_{\text{DIP,PH1}}$	0.045	mmolP m^3	Diatom half saturation constant for DIP
$Ks_{\text{DIP,PH2}}$	0.04	mmolP m^3	Flagellate half saturation constant for DIP
$Ks_{\text{DOP,PH1}}$	0.045	mmolP m^3	Diatom half saturation constant for DOP
$Ks_{\text{DOP,PH2}}$	0.04	mmolP m^3	Flagellate half saturation constant for DOP
a	0.05	No dim	Fraction of DOP available for phytoplanktonic uptake

Table 2: Parameters.

Symbol	Units	Description	Value
Si	mmol Si m^{-3}	Silicon concentration	Loureiro et al. (2009)
DOP	mmol P m^{-3}	Dissolved organic phosphorus	Loureiro et al. (2009)
R	mm $month^{-1}$	Monthly accumulated rainfall	National Institute of Meteorology
u	m s^{-1}	Wind speed	Wind measured at an automatic meteorological station 2007
$F_{(dis)}$	m^3 day^{-1}	Discharge channel flow	Literature (see section 2.2)
ρ	kg m^{-3}	Water density	Calculated from T and salinity climatologies

Table 3: Forcing variables. See Fig. 3 for details.

Growth:

$$\mathrm{Growth}_{(\mathrm{PH1})} = \mathrm{Uptake}_{(\mathrm{PH1})} \times \mathrm{LightLim}_{(\mathrm{PH1})} \tag{9}$$

$$\mathrm{Growth}_{(\mathrm{PH2})} = \mathrm{Uptake}_{(\mathrm{PH2})} \times \mathrm{LightLim}_{(\mathrm{PH2})} \tag{10}$$

$$\mathrm{Growth\_eq}_{(\mathrm{PHX})} = \mathrm{Growth}_{(\mathrm{PHX})} - \mathrm{Growth}_{(\mathrm{PHX})} \times \frac{\mathrm{Upt}_{(\mathrm{DOP,PHX})}}{\mathrm{Upt}_{(\mathrm{DOP,PHX})} + \mathrm{Upt}_{(\mathrm{DIP,PHX})}} \tag{11}$$

Light limitation:

$$\mathrm{LightLim}_{(\mathrm{PHX})} = \frac{P^B_{m(\mathrm{PHX})}\alpha_{(\mathrm{PHX})}I}{\sqrt{(P^B_{m(\mathrm{PHX})})^2 + \alpha^2_{(\mathrm{PHX})}I^2}} \tag{12}$$

$$I = PAR \times I_0 \times (1-\theta) \times \mathrm{DayLength} \tag{13}$$

Nutrient limitation:

$$\mathrm{P} = \mathrm{DIP} + \mathrm{DOP} \tag{14}$$

$$\mathrm{Uptake}_{(\mathrm{PH1})} = \frac{\mathrm{Si} \times \mathrm{DIN} \times \mathrm{P}}{\mathrm{Si} \times \mathrm{DIN} \times \mathrm{P} + K_{(\mathrm{Si,PH1})} \times \mathrm{DIN} \times \mathrm{P} + K_{(\mathrm{DIN,PH1})} \times \mathrm{Si} \times \mathrm{P} + K_{(\mathrm{P,PH1})} \times \mathrm{DIN} \times \mathrm{Si}} \tag{15}$$

$$\mathrm{Uptake}_{(\mathrm{PH2})} = \frac{\mathrm{DIN} \times \mathrm{P}}{\mathrm{DIN} \times \mathrm{P} + K_{(\mathrm{DIN,PH2})} \times \mathrm{P} + K_{(\mathrm{P,PH2})} \times \mathrm{DIN}} \tag{16}$$

$$\mathrm{Upt}_{(\mathrm{DIP,PHX})} = \frac{\mathrm{DIP}}{Ks_{(\mathrm{DIP,PHX})} + \mathrm{DIP}} \tag{17}$$

$$\mathrm{Upt}_{(\mathrm{DOP,PHX})} = (1 - \mathrm{Upt}_{(\mathrm{DIP,PHX})})\frac{a\mathrm{DOP}}{Ks_{(\mathrm{DOP,PHX})} + a\mathrm{DOP}} \tag{18}$$

Grazing:

$$\mathrm{Grazing}_{(\mathrm{PH1})} = \frac{R_m\chi_{(\mathrm{PH1})}\mathrm{PH1}^2}{Kp_{(\mathrm{PH1})}(\chi_{(\mathrm{PH2})}\mathrm{PH2} + \chi_{(\mathrm{PH1})}\mathrm{PH1}) + \chi_{(\mathrm{PH2})}\mathrm{PH2}^2 + \chi_{(\mathrm{PH1})}\mathrm{PH1}^2} \tag{19}$$

$$\mathrm{Grazing}_{(\mathrm{PH2})} = \frac{R_m\chi_{(\mathrm{PH2})}\mathrm{PH2}^2}{Kp_{(\mathrm{PH2})}(\chi_{(\mathrm{PH2})}\mathrm{PH2} + \chi_{(\mathrm{PH1})}\mathrm{PH1}) + \chi_{(\mathrm{PH2})}\mathrm{PH2}^2 + \chi_{(\mathrm{PH1})}\mathrm{PH1}^2} \tag{20}$$

Advection:

$$\text{If } \mathrm{V}_0 > 0 \quad \mathrm{Advection}_{(\mathrm{XXX})} = \frac{V_0 * ML}{A} * Ocean_{(\mathrm{XXX})} \tag{21}$$

$$\text{If } \mathrm{V}_0 < 0 \quad \mathrm{Advection}_{(\mathrm{XXX})} = \frac{V_0 * ML}{A} * \mathrm{XXX} \tag{22}$$

$$V_0 = \frac{0.0127}{\sqrt{sin|\varphi|}}u \tag{23}$$

Inputs of freshwater

$$\mathrm{FWInput}_{(\mathrm{DIX})} = \frac{F_{(dis)}C_{(dis,\mathrm{DIX})} + rF_{(und)}C_{(und,\mathrm{DIX})}}{A\ MLD} \tag{24}$$

$$r = \frac{R - min(R)}{max(R) - min(R)} + 1 \tag{25}$$

Mixed Layer Depth:

$$MLD = \sqrt{\frac{\rho L}{2\Delta\rho g}u^{\star 2}} \tag{26}$$

$$u^{\star 2} = C_D\frac{\rho_a}{\rho}u^2 \tag{27}$$

Table 4: Equations, part 1.

Sedimentation:

$$\text{Sedimentation}_{(\text{DTX})} = -\frac{\partial}{\partial z}(\phi_{(\text{DTX})}) \times \text{DTX}) \tag{28}$$

Resuspension of sediment

$$\text{when MLD(t)} \quad = 6 \quad \text{Resuspension}_{(\text{DIX,t})} = Pflow \tag{29}$$

$$\text{Resuspension}_{(\text{DIX,t+30min})} = Pflow \tag{30}$$

$$\text{Resuspension}_{(\text{DIX,t+31min})} = 0; \text{DIP} = Peq \tag{31}$$

Death:

$$\text{Death}_{(\text{XXX})} = m_{(\text{XXX})} \tag{32}$$

Excretion:

$$\text{Excretion}_{(\text{ZOO})} = E \tag{33}$$

Remineralisation:

$$\text{Remineralisation}_{(\text{DTX})} = D_{(\text{DTX})} \tag{34}$$

Table 4: Equations, part 2.

Symbol	Value	Units	Description
PH1	0.3	mmol N m^{-3}	First group of phytoplankton: diatoms
PH2	0.05	mmol N m^{-3}	Second group of phytoplankton: flagellates
ZOO	0.2	mmol N m^{-3}	Zooplankton
DIN	5.9	mmol N m^{-3}	Dissolved inorganic nitrogen
DIP	0.18	mmol P m^{-3}	Dissolved inorganic phosphorus
DTN	0.5	mmol N m^{-3}	Nitrogen fraction of the detritus
DTP	0.15	mmol P m^{-3}	Phosphorus fraction of the detritus pool

Table 5: Initial conditions

Figure1
Click here to download Table(s): figure1_caption.pdf

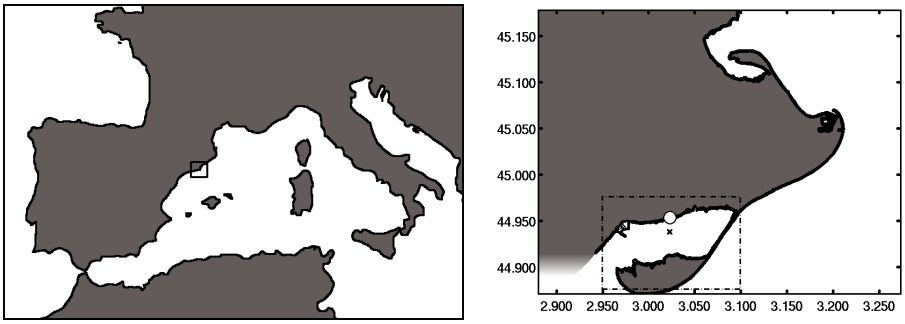

Figure 1: Map of the study zone in UTM coordinates $\times 10^5$. LEGEND: -·- Els Alfacs Bay; - - El Fangar Bay; ○ : weather station; x : sampling site.

Figure2
Click here to download Table(s): figure2_caption.pdf

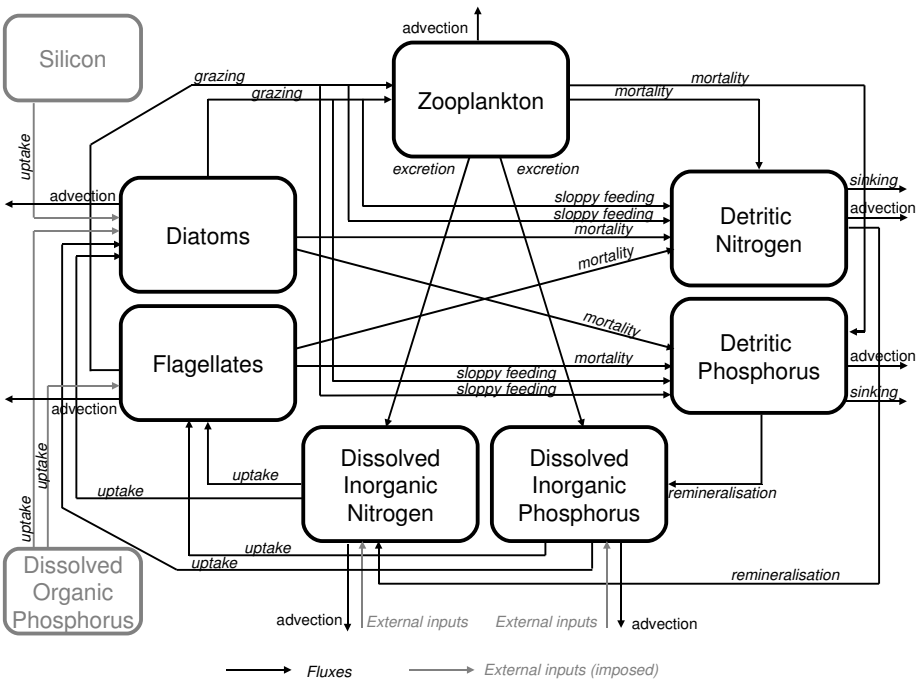

Figure 2: Diagram of the fluxes and state variables in the model.

Figure3
Click here to download Table(s): figure3_caption.pdf

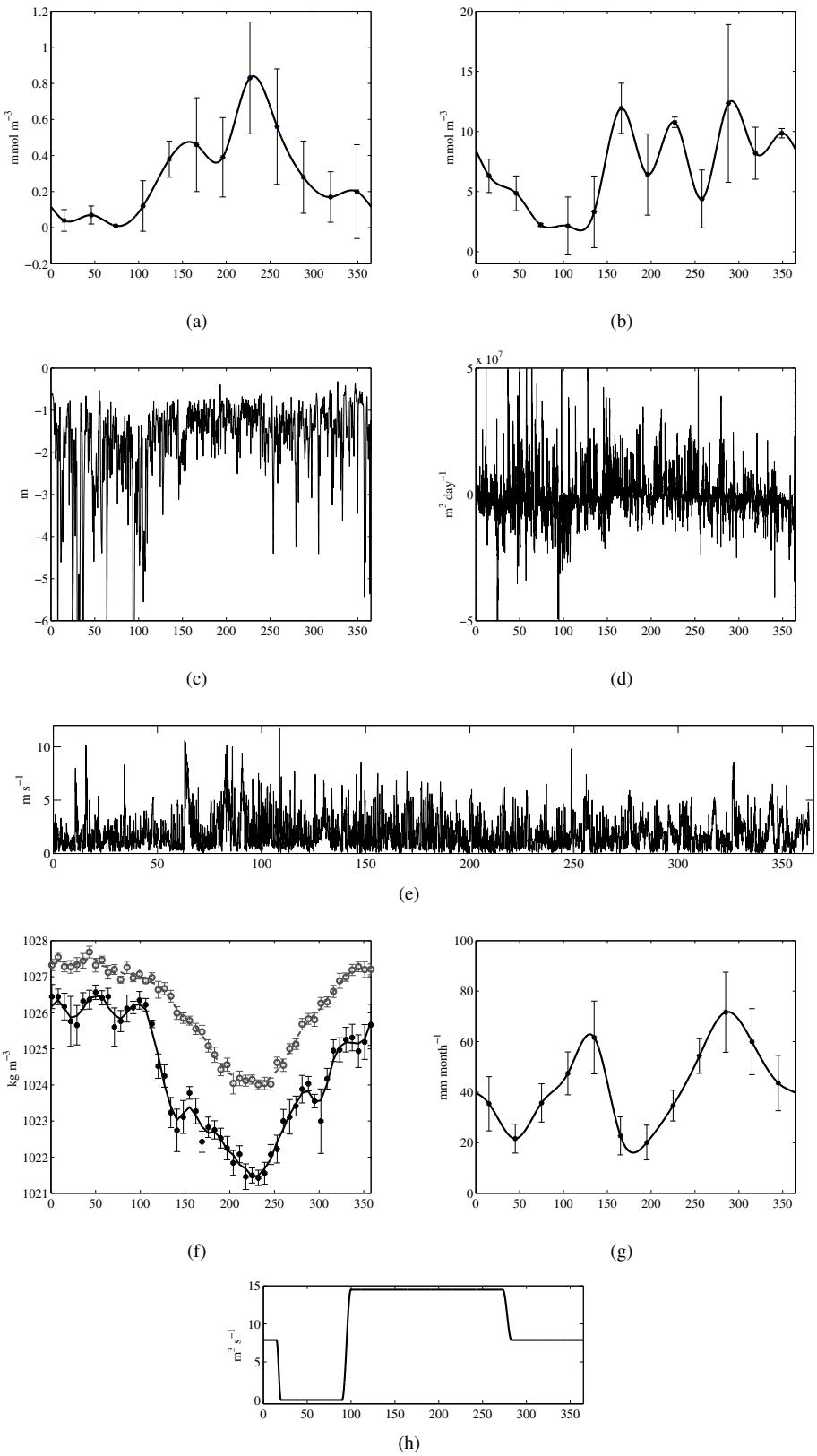

Figure 3: Forcing parameters. (a) DOP (Redrawn from Loureiro et al. (2009)) (b) Silicon (Redrawn from Loureiro et al. (2009)). (c) Mixed layer depth. See text for details about the calculation. (d) Advection flow. Positive values enter the bay. Negative values leave the bay. (e) Wind speed. (f) Density. Climatology from the period 1990-2003. Black 0.5m. Grey 5.5m. ○ weekly average. — three point average of the weekly averages. (g) Rainfall climatology. Standard deviation in the vertical bars. (h) Flux from discharge channels used in model forcing.

Figure4
Click here to download Table(s): figure4_caption.pdf

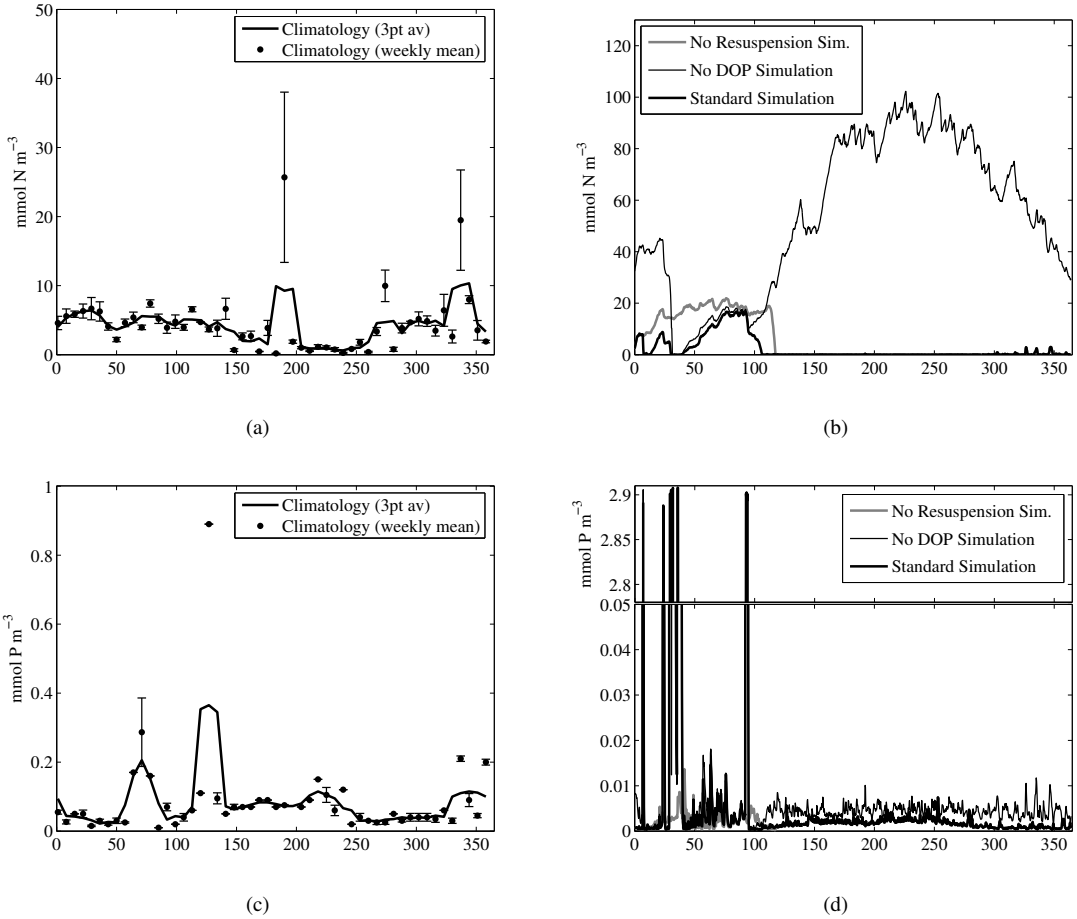

Figure 4: Observed and modeled variables for three different simulations: *Standard simulation* (including DOP use and sediments); *No Resuspension Simulation* (including DOP but not resuspension) and *No DOP Simulation* (including resuspension but not DOP). Note changes of scale. (a)Observed DIN concentration. (b)Modeled DIN concentration. (c) Observed DIP concentration. (d)Modeled DIP concentration.

Figure5
Click here to download Table(s): figure5_caption.pdf

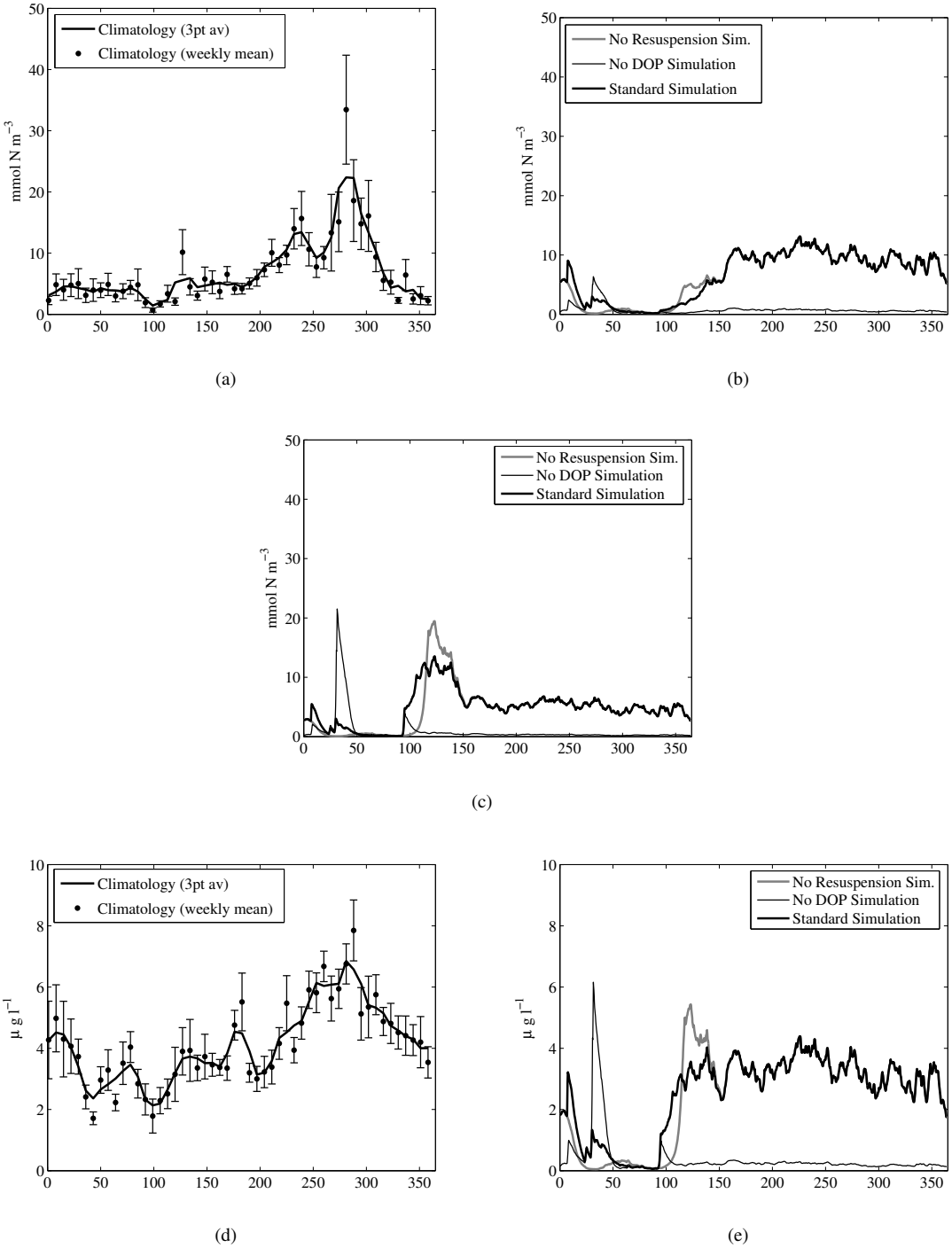

Figure 5: Observed and modeled variables for three different simulations: *Standard simulation* (including DOP use and sediments); *No Resuspension Simulation* (including DOP but not resuspension) and *No DOP Simulation* (including resuspension but not DOP). Note changes of scale. (a) Observed diatom concentration. (b) Modeled PH1 concentration. (c) Modeled PH1 concentration. (d) Observed chlorophyll *a* concentration. (e) Modeled chlorophyll *a* concentration.

Figure6
Click here to download Table(s): figure6_caption.pdf

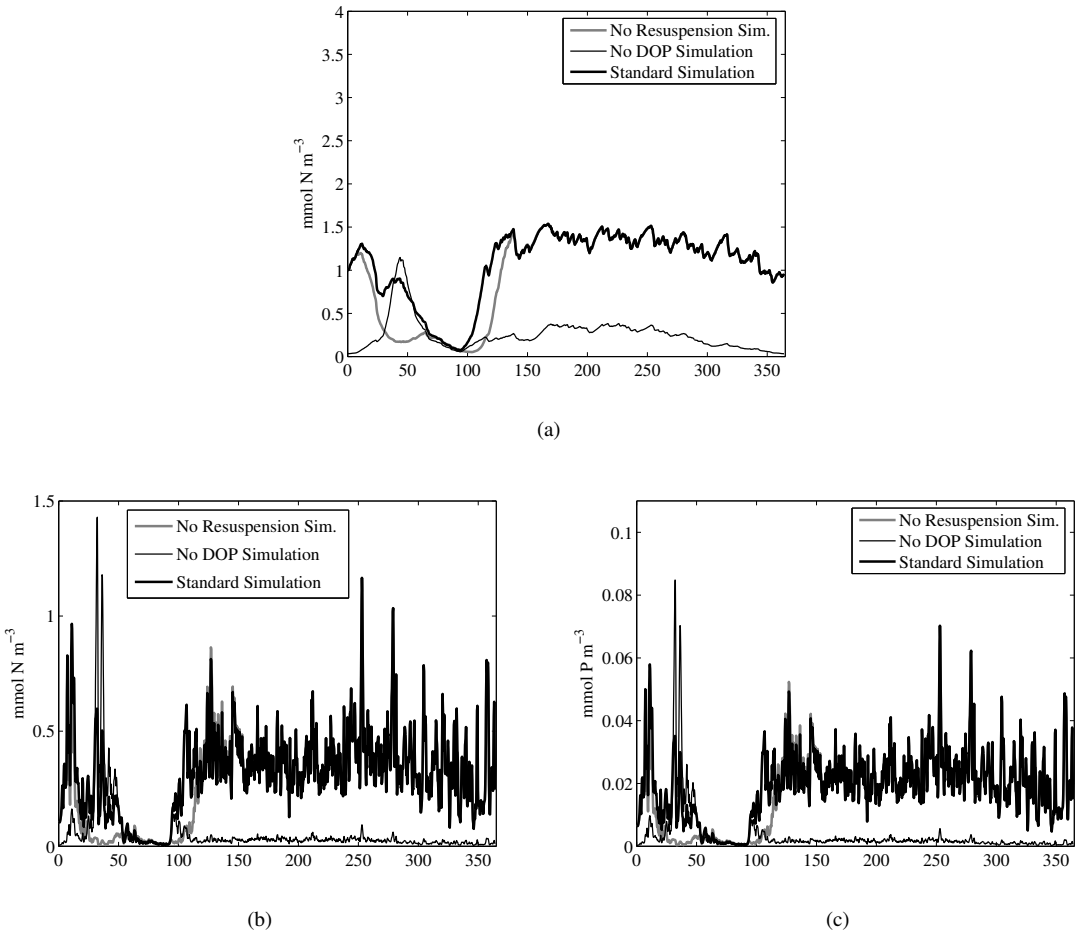

Figure 6: Modeled zooplankton and detritus for the *Standard Simulation*, the *No Resuspension Simulation* and the *No DOP Simulation*. (a) Modeled ZOO concentration (b) Modeled DTN concentration (c) Modeled DTP concentration.

Figure7
Click here to download Table(s): figure7_caption.pdf

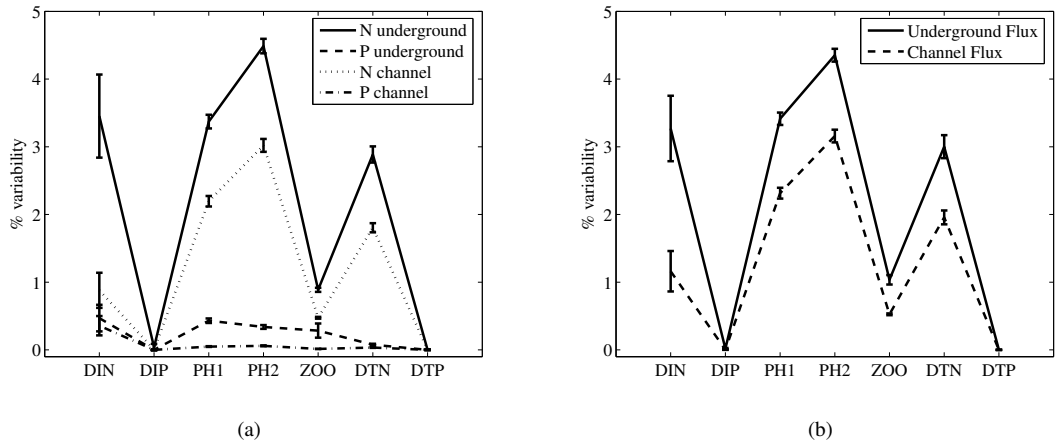

Figure 7: Mean and $\sigma/N^{\frac{1}{2}}$ of the calculated percentage of discrepancy with respect to the basic *Standard Simulation* after a 10% change of selected parameters. (a) variability of parameters of nutrient concentration in freshwater inputs: $C_{(und,DIN)}$, $C_{(und,DIP)}$,$C_{(dis,DIN)}$, $C_{(dis,DIP)}$. (b) variability of parameters of freshwater flux: $F_{(und)}$,$F_{(dis)}$.

Figure8
Click here to download Table(s): figure8_caption.pdf

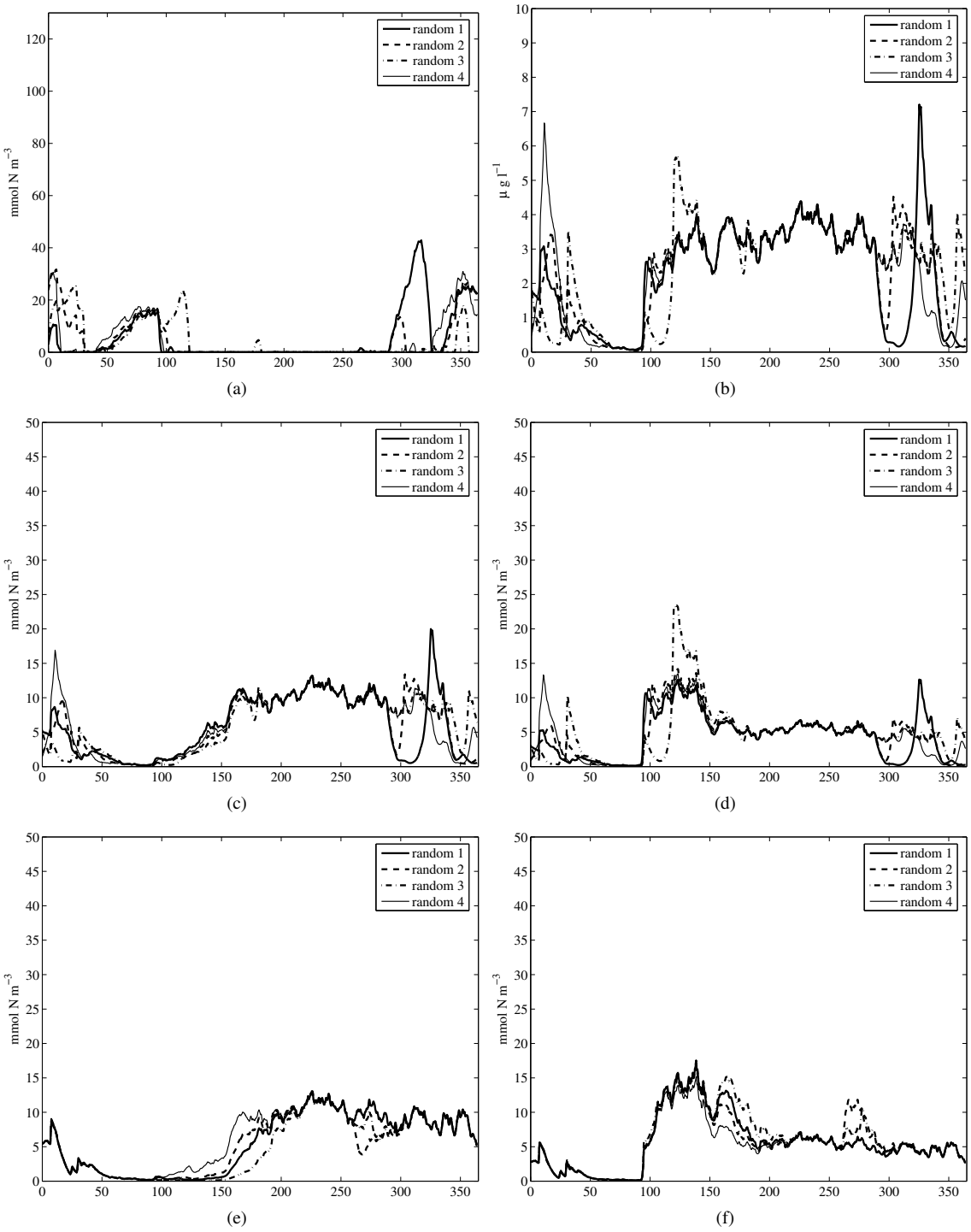

Figure 8: Results for *Standard Simulation* with the DOP and Si time series randomly modified . See section 2.4 for details. (a)DIN results for variations in DOP (b) Chlorophyll results for variations in DOP *a* (c) PH1 results for variations in DOP (d) PH2 results for variations in DOP (e) PH1 results for variations in Si (f) PH2 results for variations in Si.

Figure9
Click here to download Table(s): fiigure9_caption.pdf

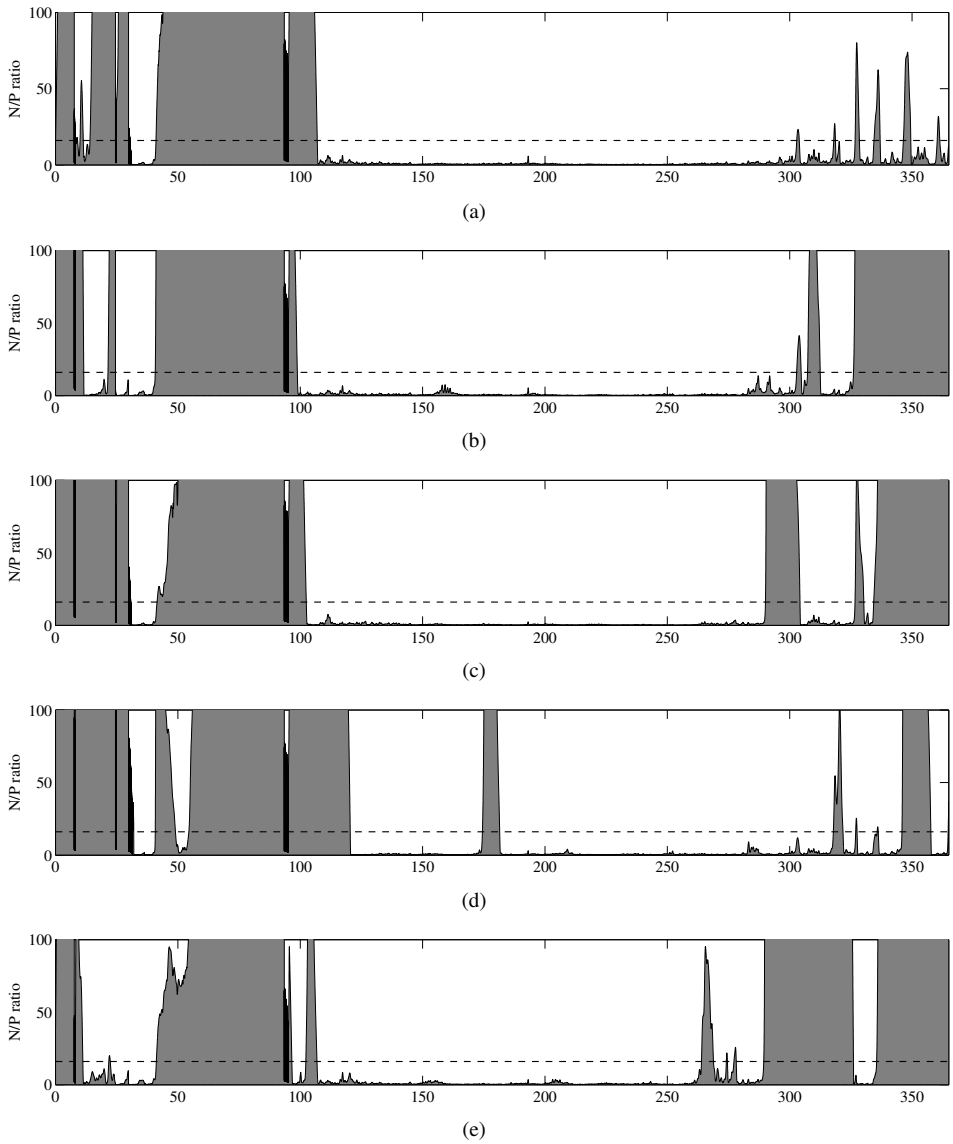

Figure 9: Variability of the DIN/(DIP+DOP) ratio in the *Standard Simulation*. Only the range 0-100 is shown. The dashed line indicates the Redfield ratio. Shaded areas above the dashed line indicate potential phosphorus limitation. (a) *Standard Simulation* (b) *Standard Simulation* with random DOP 1 (b) *Standard Simulation* with random DOP 2 (c) *Standard Simulation* with random DOP 3 (d) *Standard Simulation* with random DOP 4.